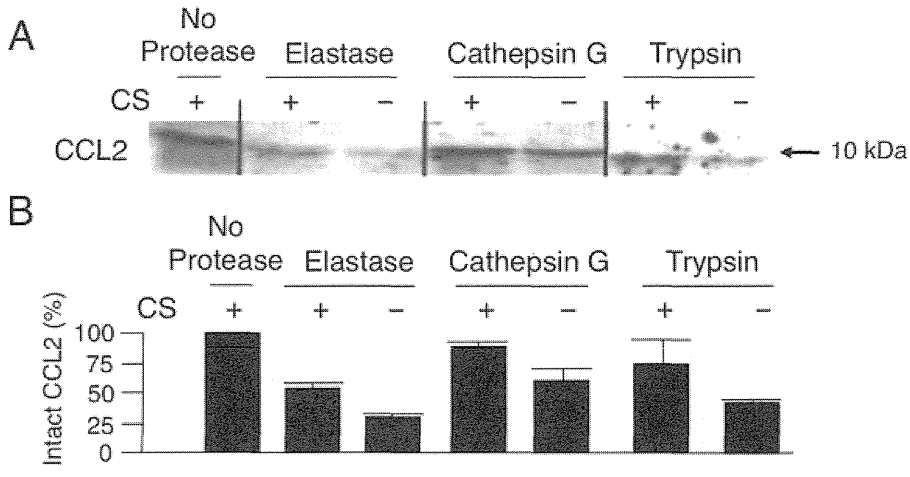

Figure 8 Binding to chondroitin sulfate chains protects CCL2 from protease-mediated degradation. **(A)** CCL2 was pre-incubated with chondroitin sulfate (CS) or vehicle, and treated with a series of proteases including elastase, cathepsin G, and trypsin. A representative immunoblot from three different experiments shows a band corresponding to intact CCL2 (10 kDa). **(B)** Amount of intact CCL2 in individual wells precoated with CS or vehicle, and subsequently treated with a series of proteases. Mean and standard deviation of three independent measurements is shown. The quantity of intact CCL2 in individual samples was expressed as a percentage of the quantity of CCL2 on wells precoated with CS and not treated with protease.

particularly noteworthy that versican generates a chemotactic gradient of CC chemokines that attracts circulating monocytes and T cells to versican-rich sites [36]. Versican subsequently promotes the adhesion and activation of recruited monocytes through binding to adhesion receptors such as integrins and CD44 on cell surfaces [37]. Through these processes, versican generates a complex set of environmental cues for infiltrating mononuclear cells and resident cells [28].

Interestingly, monocytes and monocyte-derived cells are not only recruited by versican, but are also major producers of versican [38,39]. Therefore, after migrating to versican-rich sites, these monocytes amplify the tissue response by producing more versican, which in turn promotes the influx of more monocytes [40]. In this regard, recent studies indicate that the positive feedback loop formed by versican and monocyte-lineage cells is critical for inducing certain pathologic conditions, such as tumor invasion and metastasis [41] and the formation of atherosclerotic plaques [38]. In patients with SSc, this versican-mediated positive feedback loop probably contributes to the fibrotic process by recruiting certain subsets of monocytes that acquire profibrotic properties [6,15]. The mechanisms that initially stimulate the release of versican in the early stages of SSc remain elusive, but once this positive feedback loop is established the profibrotic response would, theoretically, be amplified endlessly.

CCL2, a chemokine known to be involved in pathogenic process of SSc [42], is also elevated in circulating monocytes from SSc patients. Levels of circulating CCL2 were elevated in SSc patients, especially in those with early dcSSc [43,44] or interstitial lung disease [43,45,46]. A recent longitudinal analysis in patients with dcSSc found that circulating CCL2 decreases year after year, along with improvements in skin sclerosis [47], suggesting CCL2 as an indicator of profibrotic activity in patients with SSc. Several animal models of tissue fibrosis have demonstrated CCL2's crucial role in the fibrotic process, in which attenuating CCL2 activity prevents tissue fibrosis. Mice lacking CCL2 are protected from bleomycin-induced dermal fibrosis [48], while mice lacking the CCL2 receptor CCR2 are protected from bleomycin-induced lung fibrosis [49,50]. In these models, monocyte infiltration and collagen deposition were remarkably lower than in wild-type mice. The present study raises the question of which cell type producing CCL2 is more likely to be important for SSc pathogenesis. In this regard, abundant expression of CCL2 was observed in fibroblasts and mononuclear cells in the skin of SSc patients [45,51,52]. CCL2 has also been reported to be expressed mainly by infiltrating monocytes early in the disease, whereas fibroblasts become the major source for CCL2 in the skin later in the disease [42]. Unfortunately, our *ex vivo* analysis failed to demonstrate which cell type is the primary source of CCL2 involved in the pathogenic process of SSc.

Despite this definitive role of CCL2 in the development of excessive fibrosis *in vivo*, the details of the profibrotic mechanisms remain unclear. Yamamoto and colleagues reported that CCL2 significantly increased the levels of collagen mRNA expressed in cultured dermal fibroblasts [53], but another study failed to

reproduce this finding [54]. While CCR2 is generally not expressed by fibroblasts, Carulli and colleagues found that CCR2 is expressed by a small population of fibroblasts derived from patients with early dcSSc [55]. CCL2's profibrotic effects may thus require interaction with other cell types that express CCR2, such as monocytes and T cells. In this regard, it has been shown in SSc patients that CCL2 induces infiltrating $CD4^+$ T cells to differentiate into T-helper 2 cells, which release higher amounts of IL-4 and stimulate fibroblasts to produce excess ECM [54]. In this scenario, versican functions as a local reservoir for CCL2 and, whether bound to or released from versican, CCL2 is capable of efficiently stimulating T cells. In addition to its role in this T-cell-mediated mechanism, CCL2 also contributes to fibrotic response by promoting the migration and accumulation of profibrotic monocytes at affected sites in SSc patients. All together, the upregulation of versican and CCL2 in circulating monocytes accelerates CCL2-mediated profibrotic responses in SSc patients.

What mechanisms assist in shaping circulating monocytes to the profibrotic phenotype seen in patients with SSc? One of histopathological hallmarks of SSc is the perivascular infiltration of monocytes early in the disease [4]. It is possible that intrinsically altered monocytes migrate into target organs and trigger a profibrotic response by stimulating resident fibroblasts. Alternatively, monocyte phenotypes may be altered in SSc patients by the strong profibrotic environment. Versican production is highly regulated by soluble factors and certain stimuli, and several studies have reported that profibrotic growth factors such as transforming growth factor beta, platelet-derived growth factor, and basic fibroblast growth factor upregulate versican synthesis [56-58]. These factors are also known to upregulate CCL2 expression [59,60]. In contrast, IFNγ and IL-1β reduce versican expression [61,62]. Hypoxia dramatically upregulates versican in macrophages via hypoxia-inducible factor signaling [38]. The profibrotic and hypoxic environment associated with SSc may modulate gene expression profiles of circulating monocytes.

Genes selected by initial screening via gene expression array but excluded by confirmatory analyses may be of some interest, because some of them have been reported as molecules associated with SSc pathogenesis. For example, circulating levels of soluble L-selectin and CXCL8 were increased in SSc patients versus healthy controls [63,64]. In addition, gene expression of CCR1 was shown to be upregulated in PBMCs derived from patients with lcSSc and pulmonary arterial hypertension [65].

There are several limitations to this study. First, we used total $CD14^+$ monocytes enriched form PBMCs, which contained $CD14^+$ fibrocyte precursors [9]. Since fibrocyte precursors are reported to be a rare cell population, comprising approximately 0.5% of circulating monocytes [66], contamination of them into $CD14^+$ cells should have minimal impact on gene and protein expression data. Second, prominent upregulation of versican and CCL2 in circulating monocytes was observed in a minority of SSc patients, raising a possibility that the monocytic versican-mediated pathogenic process is only one of the roles of circulating monocytes in the pathogenesis of SSc. Since all patients with an extremely high mRNA expression level of versican had dcSSc, this type of monocyte phenotypic change might be unique to patients with a prominent fibrotic phenotype. Finally, this study represented only an *in vitro* functional interaction between versican and CCL2, which may not reflect *in vivo* activity. In addition, overexpression of versican in circulating monocytes of SSc patients might be a bystander of other more important pathogenic process of SSc. Further investigations involving genetically manipulated animals- for example, mice lacking functional versican expression specifically in monocytes - is necessary to confirm a critical role of versican upregulated by circulating monocytes in SSc pathogenesis.

Conclusion

The cellular and molecular mechanisms underlying the SSc fibrotic process primarily involve the interaction of cells such as fibroblasts, endothelial cells, and circulating immune cells, orchestrated by profibrotic soluble mediators and ECM components. This concept is supported by our observation that circulating monocytes in SSc patients are phenotypically altered and amplify a positive feedback loop, mediated by versican and CCL2, between monocytes and fibroblasts. Further studies evaluating the roles of circulating monocytes in the pathogenic process of SSc should help to elucidate the complex pathophysiology of SSc and assist us to develop novel therapeutic strategies in this multisystem fibrotic disease.

Abbreviations

CS: chondroitin sulfate; dcSSC: diffuse cutaneous systemic sclerosis; ECM: extracellular matrix: ELISA: enzyme-linked immunosorbent assay; GAG: glycosaminoglycan; IFN: interferon; IL: interleukin; lcSSc: limited cutaneous systemic sclerosis; mAb: monoclonal antibody; PBMC: peripheral blood mononuclear cell; PCR: polymerase chain reaction; RT: reverse transcriptase; SSc: systemic sclerosis.

Competing interests

The authors declare that they have no competing interests.

Authors' contributions

AM acquired: analyzed, and interpreted data, and wrote the manuscript. HY analyzed and interpreted data, and wrote the manuscript. TS, YO, and YY acquired data. MK designed the experiments, analyzed and interpreted data, and wrote the manuscript. All authors read and approved the final manuscript.

Acknowledgements
The microarray gene expression data has been deposited in the Gene Expression Omnibus database [GEO:GSE44999]. This work is supported by a research grant for Research on Intractable Diseases from the Japanese Ministry of Health, Labor, and Welfare.

Authors' details
[1]Department of Internal Medicine, Keio University School of Medicine, 35 Shinanomachi, Shunjuku, Tokyo 160-8582, Japan. [2]Yokohama City University School of Medicine, 3-9 Fukuura, Kanazawa-ku, Yokohama City, Kanagawa 236-0004, Japan.

Received: 22 October 2012 Revised: 5 April 2013
Accepted: 11 July 2013 Published: 11 July 2013

References

1. Silver RM, Medsger TA, Bolster MB: **Systemic sclerosis and scleroderma variants: clinical aspects.** In *Arthritis & Allied Conditions.* Edited by: Koopman WJ, Moreland LW. Philadelphia: Lippincott, Williams 2005:1633-1680.
2. Varga J, Abraham D: **Systemic sclerosis: a prototypic multisystem fibrotic disorder.** *J Clin Invest* 2007, **117**:557-567.
3. Ishikawa O, Ishikawa H: **Macrophage infiltration in the skin of patients with systemic sclerosis.** *J Rheumatol* 1992, **19**:1202-1206.
4. Kraaling BM, Maul GG, Jimenez SA: **Mononuclear cellular infiltrates in clinically involved skin from patients with systemic sclerosis of recent onset predominantly consist of monocytes/macrophages.** *Pathobiology* 1995, **63**:48-56.
5. Klareskog L, Gustafsson R, Scheynius A, Hallgren R: **Increased expression of platelet-derived growth factor type B receptors in the skin of patients with systemic sclerosis.** *Arthritis Rheum* 1990, **33**:1534-1541.
6. Higashi-Kuwata N, Jinnin M, Makino T, Fukushima S, Inoue Y, Muchemwa FC, Yonemura Y, Komohara Y, Takeya M, Mitsuya H, Ihn H: **Characterization of monocyte/macrophage subsets in the skin and peripheral blood derived from patients with systemic sclerosis.** *Arthritis Res Ther* 2010, **12**:R128.
7. Raes G, Beschin A, Ghassabeh GH, De Baetselier P: **Alternatively activated macrophages in protozoan infections.** *Curr Opin Immunol* 2007, **19**:454-459.
8. Tourkina E, Bonner M, Oates J, Hofbauer A, Richard M, Znoyko S, Visonti RP, Zhang J, Hatfield CM, Silver RM, Hoffman S: **Altered monocyte and fibrocyte phenotype and function in scleroderma interstitial lung disease: reversal by caveolin-1 scaffolding domain peptide.** *Fibrogenesis Tissue Repair* 2011, **4**:15.
9. Abe R, Donnelly SC, Peng T, Bucala R, Metz CN: **Peripheral blood fibrocytes: differentiation pathway and migration to wound sites.** *J Immunol* 2001, **166**:7556-7562.
10. Bucala R, Spiegel LA, Chesney J, Hogan M Cerami A: **Circulating fibrocytes define a new leukocyte subpopulation that mediates tissue repair.** *Mol Med* 1994, **1**:71-81.
11. Kuwana M, Okazaki Y, Kodama H, Izumi K, Yasuoka H, Ogawa Y, Kawakami Y, Ikeda Y: **Human circulating CD14$^+$ monocytes as a source of progenitors that exhibit mesenchymal cell differentiation.** *J Leukoc Biol* 2003, **74**:833-845.
12. Zhao Y, Glesne D, Huberman E: **A human peripheral blood monocyte-derived subset acts as pluripotent stem cells.** *Proc Natl Acad Sci USA* 2003, **100**:2426-2431.
13. Seta N, Kuwana M: **Derivation of multipotent progenitors from human circulating CD14$^+$ monocytes.** *Exp Hematol* 2010, **38**:557-563.
14. Mattoli S, Bellini A, Schmidt M: **The role of a human hematopoietic mesenchymal progenitor in wound healing and fibrotic diseases and implications for therapy.** *Curr Stem Cell Res Ther* 2009, **4**:266-280.
15. Mathai SK, Gluati M, Peng X, Russell TR, Shaw AC, Rubinowitz AN, Murray LA, Siner JM, Antin-Ozerkis DE, Montgomery RR, Reilkoff RAS, Bucala RJ, Herzog EL: **Circulating monocytes from systemic sclerosis patients with interstitial lung disease shown an enhanced profibrotic phenotype.** *Lab Invest* 2010, **90**:812-823.
16. Campioni D, Lo Monaco A, Lanza F, Moretti S, Ferrari L, Fotinidi M, La Corte R, Cuneo A, Trotta F: **CXCR4$^+$ circulating progenitor cells coexpressing monocytic and endothelial markers correlating with fibrotic clinical features are present in the peripheral blood of patients affected by systemic sclerosis.** *Haematologica* 2008, **93**:1233-1237.
17. Yamaguchi Y, Okazaki Y, Seta N, Satoh T, Takahashi K, Ikezawa Z, Kuwana M: **Enhanced angiogenic potency of monocytic endothelial progenitor cells in patients with systemic sclerosis.** *Arthritis Res Ther* 2010, **12**:R205.
18. Duan H, Fleming J, Pritchard DK, Amon LM, Xue J Arnett HA, Chen G, Breen P, Buchner JH, Molitor JA, Elkon KB, Schwartz SM: **Combined analysis of monocytes and lymphocytes messenger RNA expression with serum protein profiles in patients with scleroderma.** *Arthritis Rheum* 2008, **58**:1465-1474.
19. York MR, Nagai T, Mangini AJ, Lemaire R, van Seventer JM, Lafyatis R: **A macrophage marker, Siglec-1, is increased on circulating monocytes in patients with systemic sclerosis and induced by type I interferons and Toll-like receptor agonists.** *Arthritis Rheum* 2007, **56**:1010-1020.
20. Binai N, O'Reilly S, Griffiths B, van Laar JM, Hügle T: **Differentiation potential of CD14$^+$ monocytes into myofibroblasts in patients with systemic sclerosis.** *PLoS One* 2012, **7**:e33508.
21. Subcommittee for Scleroderma Criteria of the American Rheumatism Association Diagnostic and Therapeutic Criteria Committee: **Preliminary criteria for the classification of systemic sclerosis (scleroderma).** *Arthritis Rheum* 1980, **23**:581-590.
22. Medsger TA Jr: **Systemic sclerosis (scleroderma), localized scleroderma, eosinophilic fasciitis and calcinosis.** In *Arthritis and Allied Conditions: A Textbook of Rheumatology..* 11 edition. Edited by: McCarty. Philadelphia: Lea 1989:1118-1165.
23. Kuwana M, Kaburaki J, Okano T, Tojo T, Homma M: **Clinical and prognostic associations based on serum antinuclear antibodies in Japanese patients with systemic sclerosis.** *Arthritis Rheum* 1994, **37**:75-83.
24. Kodama H, Inoue T, Watanabe R, Yasuoka H, Kawakami Y, Ogawa S, Ikeda Y, Mikoshiba K, Kuwana Y: **Cardiomyogenic potential of mesenchymal progenitors derived from human circulating CD14$^+$ monocytes.** *Stem Cells Dev* 2005, **14**:676-686.
25. Frommer KW, Reichenmiller K, Schutt BS, Hoeflich A, Ranke MB, Dodt G, Elmilinger MW: **IGF-independent effects of IGFBP-2 on the human breast cancer cell line Hs578T.** *J Mol Endocrinol* 2006, **37**:13-23.
26. Yasuoka H, Yamaguchi Y, Feghali-Bostwick CA: **IGFBP-5 induces fibroblasts and peripheral blood mononuclear cell migration and regulated by MAPK signaling in vitro.** *Am J Respir Cell Mol Biol* 2009, **41**:179-188.
27. Yasuoka H, Zhou Z, Pilewski JM, Oury TD, Choi AMK, Feghali-Bostwick CA: **IGFBP-5 induces pulmonary fibrosis and triggers mononuclear cellular infiltration.** *Am J Pathol* 2006, **169**:1633-1642.
28. Wight TN: **Versican: a versatile extracellular matrix proteoglycan in cell biology.** *Curr Opin Cell Biol* 2002, **14**:617-623.
29. Hoogewerf AJ, Kuschert GS, Proudfoot AE, Borlat F, Clark-Lewis I, Power CA, Wells TN: **Glycosaminoglycans mediate cell surface oligomerization of chemokines.** *Biochemistry* 1997, **36**:13570-13578.
30. Prydz K, Dalen KT: **Synthesis and sorting of proteoglycans.** *J Cell Sci* 2000, **113(Pt 2)**:193-205.
31. Deshmane SL, Kremlev S, Amini S, Sawaya BE: **Monocyte chemoattractant protein 1 (MCP-1): an overview.** *J Interferon Cytokine Res* 2009, **29**:313-326.
32. Zimmermann DR, Dours-Zimmermann MT: **Extracellular matrix of the central nervous system: from neglect to challenge.** *Histochem Cell Biol* 2008, **130**:635-653.
33. Seidelmann SB, Kuo C, Pleskac N, Molina J, Sayers S, Li R, Zhou J, Johnson P, Braun K, Chan C, Teupser D, Breslow JL, Wight TN, Tall AR, Welch CL: **Athsq1 is an atherosclerosis modifier locus with dramatic effects on lesion area and prominent accumulation of versican.** *Arterioscler Thromb Vasc Biol* 2008, **28**:2180-2186.
34. Suwiwat S, Ricciardelli C, Tammi R, Tammi M, Auvinen P, Kosma VM, LeBaron RG, Raymond WA, Tilley WD, Horsfall DJ: **Expression of extracellular matrix components versican, chondroitin sulfate, tenascin, and hyaluronan, and their association with disease outcome in node-negative breast cancer.** *Clin Cancer Res* 2004, **10**:2491-2498.
35. Hesselstrand R, Westergren-Thorsson G, Scheja A, Wildt M, Akesson A: **The association between changes in skin echogenicity and the fibroblasts production of biglycan and versican in systemic sclerosis.** *Clin Exp Rheumatol* 2002, **20**:301-308.
36. Kawashima H, Atarashi K, Hirose M, Hirose J, Yamada S, Sugahara K, Miyasaka M: **Oversulfated chondroitin/dermatan sulfates containing GlcAb1/IdoAa1-3GalNac (4,6-O-disulfate) interact with L- and P-selectin and chemokines.** *J Biol Chem* 2002, **277**:12921-12930.
37. Wu YJ, La Pierre DP, Wu J, Yee AJ, Yang BB: **The interaction of versican with its binding partners.** *Cell Res* 2005, **15**:483-494.

38. Asplund A, Stillemark-Billton P, Larsson E, Rydberg EK, Moses J, Hultén LM, Fagerberg B, Camejo G, Bondjers G: **Hypoxic regulation of secreted proteoglycans in macrophages.** *Glycobiology* 2010, **20**:33-40.
39. Makatsori E, Lamari FN, Theocharis AD, Anagnostides S, Hjerpe A, Tsegenidis T, Karamanos NK: **Large matrix proteoglycans, versican and perlecan, are expressed and secreted by human leukemic monocytes.** *Anticancer Res* 2003, **23**:3303-3309.
40. Hirose J, Kawashima H, Yoshie O, Tashiro K, Miyasaka M: **Versican interacts with chemokines and modulates cellular responses.** *J Biol Chem* 2001, **276**:5228-5234.
41. Said N, Sanchez-Carbayo M, Smith SC, Theodorescu D: **RhoGDI2 suppresses lung metastasis in mice by reducing tumor versican expression and macrophage infiltration.** *J Clin Invest* 2012, **122**:1502-1518.
42. Distler JH, Akhmetshina A, Schett G, Distler O: **Monocyte chemoattractant proteins in the pathogenesis of systemic sclerosis.** *Rheumatology* 2009, **48**:98-103.
43. Carulli MT, Handler C, Coghlan JG, Black CM, Denton CP: **Can CCL2 serum levels be used in risk stratification or to monitor treatment response in systemic sclerosis?** *Ann Rheum Dis* 2008, **67**:105-109.
44. Peterlana D, Puccetti A, Caramaschi P, Biasi D, Beri R, Simeoni S, Corrocher R, Lunardi C: **Endothelin-1 serum levels correlate with MCP-1 but not with homocysteine plasma concentration in patients with systemic sclerosis.** *Scand J Rheumatol* 2006, **35**:133-137.
45. Hasegawa M, Sato S, Takehara K: **Augmented production of chemokines (monocyte chemotactic protein-1 (MCP-1), macrophage inflammatory protein-1alpha (MIP-1α) and MIP-1β) in patients with systemic sclerosis: MCP-1 and MIP-1α may be involved in the development of pulmonary fibrosis.** *Clin Exp Immunol* 1999, **117**:159-165.
46. Scala E, Pallotta S, Frezzolini A, Abeni D, Barbieri C, Sampgna F De Pita O, Paganelli R, Russo G: **Cytokine and an chemokine levels in systemic sclerosis: relationship with cutaneous and internal organ involvement.** *Clin Exp Immunol* 2004, **138**:540-546.
47. Hasegawa M, Fujimoto M, Matsushita T, Hamaguchi Y, Takehara K, Sato S: **Serum chemokine and cytokine levels as indicators of disease activity in patients with systemic sclerosis.** *Clin Rheumatol* 2011, **30**:231-237.
48. Ferreira AM, Takagawa S, Fresco R, Zhu X, Varga J, DiPietro LA: **Diminished induction of skin fibrosis in mice with MCP-1 deficiency.** *J Invest Dermatol* 2006, **126**:1900-1908.
49. Okuma T, Terasaki Y, Kakita K Kobayashi H, Kuziel WA, Kawasuji M, Takeya M: **C-C chemokine receptor 2 (CCR2) deficiency improves bleomycin-induced pulmonary fibrosis by attenuation of both macrophage infiltration and production of macrophage-derived matrix metalloproteinases.** *J Pathol* 2004, **204**:594-604.
50. Moore B, Paine R, Christensen PJ, Moore TA, Sitterding S, Ngan R, Wilke CA, Kuziel WA, Toews GB: **Protection from pulmonary fibrosis in the absence of CCR2 signaling.** *J Immunol* 2001, **167**:4368-4377.
51. Distler O, Pap T, Kowal-Bielecka O Meyringer R, Guiducci S, Landthaler M, Schölmerich J, Michael BA, Gay RE, Matucci-Cerinic M, Gay S, Müller-Ladner U: **Overexpression of monocyte chemoattractant protein 1 in systemic sclerosis: role of platelet-derived growth factor and effects on monocyte chemotaxis and collagen synthesis.** *Arthritis Rheum* 2001, **44**:2665-2678.
52. Galindo M, Santiago G, Rivero M, Rullas J, Alcami J, Pablos JL: **Chemokine expression by systemic sclerosis fibroblasts: abnormal regulation of monocyte chemotactic protein-1 (MCP-1) expression.** *Arthritis Rheum* 2001, **44**:1382-1386.
53. Yamamoto T, Eckes B, Krieg T: **Effect of interleukin-10 on the gene expression of type I collagen, fibronectin, and decorin in human skin fibroblasts: differential regulation by transforming growth factor-beta and monocyte chemoattractant protein-1.** *Biochem Biophys Res Commun* 2001, **281**:200-205.
54. Distler JHW, Jungle A, Caretto D, Schulze-Horsel U, Kowal-Bielecka O, Gay RE, Michel BA, Muller-Ladner U, Kalden JR, Gay S, Distler O: **Monocyte chemoattractant protein 1 released from glycosaminoglycans mediates its profibrotic effects in systemic sclerosis via the release of interleukin-4 from T cells.** *Arthritis Rheum* 2006, **54**:214-225.
55. Carulli MT, Ong VH, Ponticos M, Shiwen X, Abraham DJ, Black CM, Denton CP: **Chemokine receptor CCR2 expression by systemic sclerosis fibroblasts: evidence for autocrine regulation of myofibroblast differentiation.** *Arthritis Rheum* 2005, **52**:3772-3782.
56. Kahari CM, Larjava H, Uitto J: **Differential regulation of extracellular matrix proteoglycan (PG) gene expression: transforming growth factor β1 up-regulates biglycan (PGI), and versican (large fibroblast PG) but down-regulates decorin mRNA in human fibroblasts in culture.** *J Biol Chem* 1991, **266**:10608-10615.
57. Norian JM, Malik M, Parker CY, Joseph D, Leppert PC, Segars JH, Catherino WH: **Transforming growth factor β3 regulates the versican variants in the extracellular matrix-rich uterine leiomyomas.** *Reprod Sci* 2009, **16**:1153-1164.
58. Schönherr E, Kinsella MG, Wight TN: **Genistein selectively inhibits platelet-derived growth factor-stimulated versican biosynthesis in monkey arterial smooth muscle cells.** *Arch Biochem Biophys* 1997, **339**:353-361.
59. Qi W, Chen X, Polhill TS, Sumual S, Twigg S, Gilbert RE, Pollock CA: **TGF-β1 induces IL-8 and MCP-1 through a connective tissue growth factor-independent pathway.** *Am J Physiol Renal Physiol* 2006, **290**:F703-F709.
60. Bsoul S, Terezhalmy G, Abboud H, Woodruff K, Abboud SL: **PDGF-BB and bFGF stimulate DNA synthesis and upregulate CSF-1 and MCP-1 gene expression in dental follicle cells.** *Arch Oral Biol* 2003, **48**:459-465.
61. Lemire JM, Chan CK, Bressler S, Miller J, LeBaron RG, Wight TN: **Interleukin-1β selectively decreases the synthesis of versican by arterial smooth muscle cells.** *J Cell Biochem* 2007, **101**:753-766.
62. Venkatesan N, Roughley PJ, Ludwig MS: **Proteoglycan expression in bleomycin lung fibroblasts: role of transforming growth factor-β1 and interferon-γ.** *Am J Physiol Lung Cell Mol Physiol* 2002, **283**:L806-L814.
63. Dunne JV, van Eeden SF, Keen KJ: **L-selectin and skin damage in systemic sclerosis.** *PLoS One* 2012, **7**:e44814.
64. Colludo V, Baldwin HM, Singh MD, Fraser AR, Wilson C, Gilmour A, Hueber AJ, Bonino C, McInnes IB, Montecucco C, Graham GJ: **An investigation of the inflammatory cytokine and chemokine network in systemic sclerosis.** *Ann Rheum Dis* 2011, **70**:1115-1121.
65. Pendergrass SA, Hayes E, Farina G, Lemaire R, Farber HW, Whitfield ML, Rafyatis R: **Limited systemic sclerosis patients with pulmonary arterial hypertension show biomarkers of inflammation and vascular injury.** *PLoS One* 2010, **17**:e21206.
66. Bucala R: **Fibrocytes and fibrosis.** *Q J Med* 2012, **105**:505-508.

doi:10.1186/ar4251
Cite this article as: Masuda *et al.*: Versican is upregulated in circulating monocytes in patients with systemic sclerosis and amplifies a CCL2-mediated pathogenic loop. *Arthritis Research & Therapy* 2013 15:R74.

PLOS ONE

Platelet-Derived Stromal Cell-Derived Factor-1 Is Required for the Transformation of Circulating Monocytes into Multipotential Cells

Noriyuki Seta[1], Yuka Okazaki[1], Hiroshi Miyazaki[2], Takashi Kato[1,3], Masataka Kuwana[1]*

1 Division of Rheumatology, Department of Internal Medicine, Keio University School of Medicine, Tokyo, Japan, **2** Innovative Drug Research Laboratories, Research Division, Kyowa Hakko Kirin Co., Ltd., Takasaki, Japan, **3** Department of Biology, School of Education, Waseda University, Tokyo, Japan

Abstract

Background: We previously described a primitive cell population derived from human circulating $CD14^+$ monocytes, named monocyte-derived multipotential cells (MOMCs), which are capable of differentiating into mesenchymal and endothelial lineages. To generate MOMCs *in vitro,* monocytes are required to bind to fibronectin and be exposed to soluble factor(s) derived from circulating $CD14^-$ cells. The present study was conducted to identify factors that induce MOMC differentiation.

Methods: We cultured $CD14^+$ monocytes on fibronectin in the presence or absence of platelets, $CD14^-$ peripheral blood mononuclear cells, platelet-conditioned medium, or candidate MOMC differentiation factors. The transformation of monocytes into MOMCs was assessed by the presence of spindle-shaped adherent cells, CD34 expression, and the potential to differentiate *in vitro* into mesenchymal and endothelial lineages.

Results: The presence of platelets or platelet-conditioned medium was required to generate MOMCs from monocytes. A screening of candidate platelet-derived soluble factors identified stromal cell-derived factor (SDF)-1 as a requirement for generating MOMCs. Blocking an interaction between SDF-1 and its receptor CXCR4 inhibited MOMC generation, further confirming SDF-1's critical role in this process. Finally, circulating MOMC precursors were found to reside in the $CD14^+CXCR4^{high}$ cell population.

Conclusion: The interaction of SDF-1 with CXCR4 is essential for the transformation of circulating monocytes into MOMCs.

Citation: Seta N, Okazaki Y, Miyazaki H, Kato T, Kuwana M (2013) Platelet-Derived Stromal Cell-Derived Factor-1 Is Required for the Transformation of Circulating Monocytes into Multipotential Cells. PLoS ONE 8(9): e74246. doi:10.1371/journal.pone.0074246

Editor: Carol Feghali-Bostwick, University of Pittsburgh, United States of America

Received April 23, 2013; **Accepted** July 31, 2013; **Published** September 16, 2013

Funding: This work was supported by the New Energy and Industrial Technology Development Organization in Japan. The funders had no role in study design, data collection and analysis, decision to publish, or preparation of the manuscript.

Competing Interests: Masataka Kuwana, the corresponding author, currently serves as an Academic Editor of PLOS ONE. Hiroshi Miyazaki is an employee of Kyowa Hakko Kirin Co., Ltd. There are no patents, products in development or marketed products to declare. This does not alter the authors' adherence to all the PLOS ONE policies on sharing data and materials.

* E-mail: kuwanam@z5.keio.jp

Introduction

Circulating $CD14^+$ monocytes, which are heterogeneous in terms of surface markers, phagocytic capacity, and differentiation potential, are committed precursors in transit from the bone marrow to their ultimate site of activity [1]. Until recently, it was believed that monocytes could only differentiate into cells with phagocytic capacity such as macrophages, and dendritic cells [1–3]. However, there is growing evidence that circulating monocytes can differentiate into a variety of cell types in addition to phagocytes [4–8]. We previously identified a peripheral blood-derived cell population, termed monocyte-derived multipotential cells (MOMCs), that have a fibroblast-like morphology in culture and a unique phenotype positive for CD14, CD45, CD34, and type I collagen [9]. This population originates from circulating $CD14^+$ monocytes, and contains primitive cells that can differentiate into cells with the typical phenotypes and functions of mesenchymal cells, neurons, and endothelium *in vitro* [8–12]. We recently showed that the intracranial delivery of MOMCs enhances functional recovery in a rat model for ischemic stroke [13]. On the other hand, MOMCs derived from patients with systemic sclerosis were functionally altered and deficient in their ability to differentiate into endothelial cells, either *in vitro* or *in vivo* [14]. These findings raised the possibility that circulating monocytes may contribute to tissue remodeling and regeneration through MOMC differentiation in physiologic and pathogenic states.

MOMCs are obtained with a 7-day culture of peripheral blood mononuclear cells (PBMCs) on fibronectin-coated plastic plates with 10% fetal bovine serum (FBS) as the only source of growth factors. Our previous research indicated that to generate MOMCs from circulating $CD14^+$ monocytes *in vivo*, the monocytes are required to bind to fibronectin's RGD domain via $\alpha_5\beta_1$ integrin on the monocytes' cell surface, and are required to be exposed to soluble factor(s) derived from the circulating $CD14^-$ cell fraction [9,15]. However, the details of the molecular factors involved in this process remain unknown. In this study, we examined

molecular factors involved in MOMC differentiation by focusing on soluble factor(s) derived from circulating $CD14^-$ cells.

Materials and Methods

Cell Preparations

PBMCs were isolated from heparinized venous blood from 10 healthy volunteers, aged 22–38, using Lymphoprep (Axis-Shield PoC AS, Oslo, Norway) density-gradient centrifugation. In some experiments, 3.8% sodium citrate was used as an anticoagulant instead of heparin. Since the PBMC fraction was contaminated with a large number of platelets, we removed platelets from the PBMC fraction by MACS column separation using anti-CD61 monoclonal antibody (mAb)-coupled magnetic beads (Miltenyi Biotech, Bergisch Gladbach, Germany). The platelet-depleted PBMCs were then divided into $CD14^+$ monocytes and $CD14^-$ PBMCs by MACS column separation using anti-CD14 mAb-coupled magnetic beads (Miltenyi Biotech). In some instances, the $CD14^+$ monocytes were separated into two distinct populations based on high or low CXCR4 expression, by fluorescence-activated cell sorting. Specifically, $CD14^+$ monocytes were incubated with PE-conjugated anti-CXCR4 mAb (BD Biosciences, San Diego, CA) or FITC-conjugated anti-CD11a mAb (Beckman-Coulter, Fullerton, CA) in combination with PC5-conjugated anti-CD14 mAb (Miltenyi Biotech), and were sorted with a FACS® Calibur system. The $CD14^+$ cells with CXCR4 levels in the top and bottom 40% were used as $CD14^+CXCR4^{high}$ and $CD14^+CXCR4^{low}$ cells, respectively. $CD14^+CD11a^+$ cells were also isolated as a control for the sorting procedure.

Platelets were prepared from platelet-rich plasma by a gel-filtration method described elsewhere [16], with modifications to avoid activating the platelets during the isolation procedure. Briefly, sterilized Sepharose CL-2B gel (GE Healthcare Biosciences AB, Uppsala, Sweden) in phosphate buffer (0.1 M $NaH_2PO_4 \cdot 2H_2O$, adjusted to pH 7 with NaOH) was washed and equilibrated with Tyrodes buffer (140 mM NaCl, 3 mM KCl, 1 mM $MgCl_2$, 16.62 mM $NaHCO_3$, pH 7.4, 5.5 mM glucose, and 10 mM HEPES) containing 0.5% bovine serum albumin (BSA) (Sigma, St. Luis, MO). After packing the Sepharose beads into a column, Tyrodes buffer containing 0.5% BSA was replaced with serum-free low-glucose Dulbecco's modified Eagle's medium (DMEM; Sigma). Platelet-rich plasma was prepared from peripheral blood by centrifugation (120 g for 10 minutes) and gently applied to the Sepharose column. Platelets were then collected in clouded drips before the plasma proteins exited the column.

The concentration of isolated cells was determined by counting the cells under an inverted microscope (IX81: Olympus, Tokyo, Japan). The protocol of this study was approved by the Ethics Committee of Keio University School of Medicine. All blood samples were obtained from subjects who had given written informed consent.

Preparation of Platelet-Conditioned Medium

Platelet-conditioned medium was prepared from autologous platelets by several methods. Platelets (4×10^7/mL) in low-glucose DMEM containing 10% FBS (JRH Bioscience, Lenexa, KS) were cultured on plastic plates coated with fibronectin (Sigma) for 24 hours, and supernatants recovered by centrifugation (180 g for 10 minutes) were used directly as platelet-conditioned medium. Alternatively, platelets (2.5×10^8/mL) in serum-free low-glucose DMEM were stimulated with one of the following platelet agonists: thrombin (1 U/mL; Mochida Pharmaceutical Co., Ltd., Tokyo, Japan), thrombin receptor activation peptide (SFLLRN; 50 μM), type I collagen (4 μg/mL), adenosine diphosphate (ADP; 400 μM), ristocetin (15 mg/mL), or epinephrine (50 μM) (Sigma) at 37°C for 15 minutes. Supernatants prepared by centrifugation and diluted 10 times with low-glucose DMEM containing 10% FBS were also used as platelet-conditioned medium. In some experiments, medium conditioned by thrombin-treated platelets was fractionated using an Ultrafree-MC Centrifugal Filter® (Millipore, Bedford, MA) with a 30-kDa nominal MW limit, resulting in media enriched in either proteins with a molecular weight (MW) greater than 30 kDa, or with proteins with an MW less than 30 kDa.

Cultures for Generating MOMCs

In the original method, MOMCs are generated by culturing PBMCs (2×10^6/mL) for 7 days in low-glucose DMEM containing 10% FBS on fibronectin-coated plastic plates, without any additional growth factors [9]. To evaluate the cell populations and soluble factors required to transform circulating monocytes into MOMCs, sorted $CD14^+$ monocytes (2×10^5/mL) were cultured on fibronectin-coated plastic plates with or without autologous platelets (4×10^7/mL), $CD14^-$ PBMCs (10^6 cells/mL), or unfractionated or fractionated platelet-conditioned medium. In addition, $CD14^+$ monocytes were cultured on fibronectin-coated plastic plates in low-glucose DMEM containing 10% FBS, in the presence or absence of serial concentrations of the following: interleukin (IL)-7, epidermal growth factor (EGF), basic fibroblast growth factor (bFGF), transforming growth factor-β (TGF-β), platelet-derived growth factor (PDGF)-AA, PDGF-AB, IL-8, growth-related oncogene-α (GRO-α), epithelial cell-derived neutrophil-activating peptide 78 (ENA78), thymus and activation-regulated chemokine (TARC), stromal cell-derived factor (SDF)-1, platelet factor 4 (PF4), regulated upon activation, normal T cell expressed and secreted (RANTES), macrophage inflammatory protein-1α (MIP-1α), monocyte chemotactic protein-3 (MCP-3), or neutrophil-activating peptide 2 (NAP2). All of these cytokines, growth factors, and chemokines were purchased from R&D Systems (Minneapolis, MN, USA). In some instances, AMD 3100 (Sigma) was added to the MOMC generation culture at a final concentration of 0, 1, or 5 ng/mL.

In all cultures, medium containing floating cells was exchanged with fresh low-glucose DMED with 10% FBS on day 3. The number and morphology of adherent cells was assessed under an inverted microscope on day 7. The number of total and spindle-shaped adherent cells in a 1 mm x 1 mm square was counted on 10 randomly selected fields, and the efficacy of adherent cell generation was expressed as the proportion (%) of the number of the cells of interest in the culture compared to those observed in a culture of $CD14^+$ monocytes alone, in low-glucose DMEM containing 10% FBS during the entire culture period. In experiments using $CD14^+CXCR4^{high}$ and $CD14^+CXCR4^{low}$ cells, the results were expressed in comparison with $CD14^+CD11a^+$ cell cultures. The adherent cells were subsequently recovered with 0.25% trypsin and assayed for cell-surface phenotype and *in vitro* differentiation capacity.

Flow Cytometric Analysis

After staining with FITC-conjugated anti-CD34, FITC-conjugated anti-CD11a or PE-conjugated anti-CXCR4 mAb in combination with PC5-conjugated anti-CD14 mAb, cells were analyzed on a FACS® Calibur flow cytometer using CellQuest software (BD Biosciences). Viable cells were identified by gating based on forward and side scatters, and data were shown as logarithmic dot-plots or histograms.

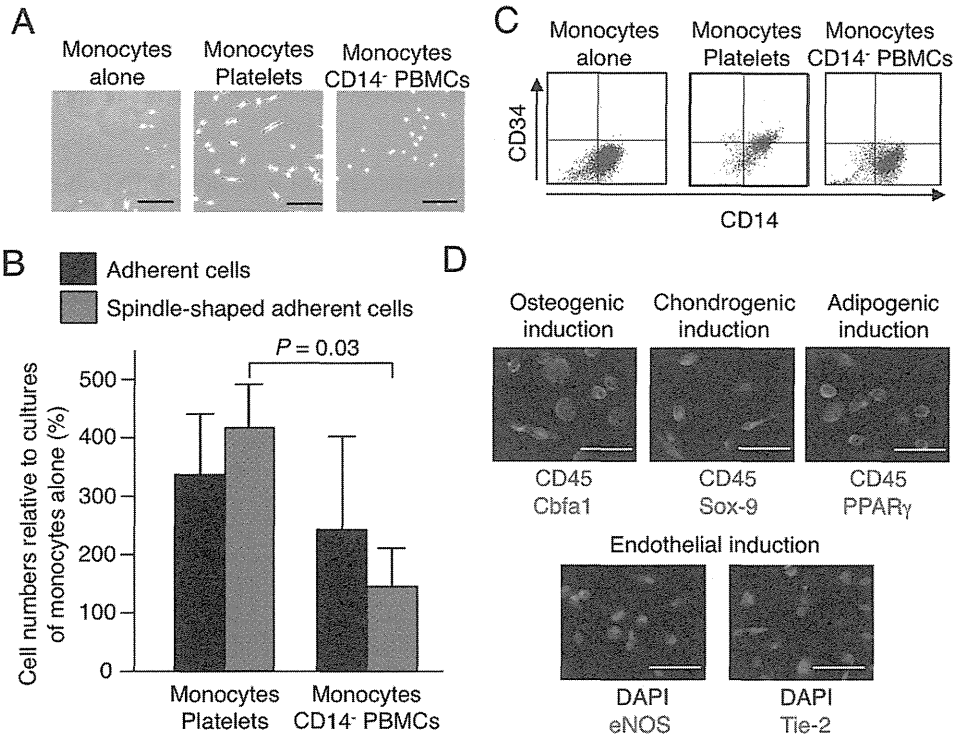

Figure 1. Platelets are required for the generation of MOMCs. $CD14^+$ monocytes were cultured on fibronectin with platelets or platelet-depleted $CD14^-$ PBMCs, or on fibronectin alone. (**A**) Morphology of adherent cells on culture day 7. Bars: 200 μm. (**B**) The total number of cells and the number of spindle-shaped adherent cells generated are expressed in proportion (%) to those generated by monocyte culture alone. The results shown are the mean and SD of three independent experiments. (**C**) Cell-surface CD14 and CD34 expression on the cultured adherent cells, as analyzed by flow cytometry. (**D**) The multidifferentiation potential of adherent cells obtained by culturing monocytes and platelets. Cells treated for osteogenic, chondrogenic, adipogenic, and endothelial induction for 1 week were analyzed by immunohistochemical staining for Cbfa1, Sox-9, or PPARγ (red) in combination with CD45 (green), or for eNOS or Tie-2 (red) in combination with DAPI (blue), and were observed under a fluorescence microscope. Representative results of three independent experiments are shown. Bars: 50 μm.
doi:10.1371/journal.pone.0074246.g001

Capacity for *In Vitro* Differentiation into Mesenchymal and Endothelial Lineages

Adherent cells obtained in various MOMC generation cultures were replated on fibronectin-coated chamber slides (BD Biosciences) in high-glucose DMEM containing 10% FBS, and were grown to semi-confluence. The cells were then cultured under conditions known to induce the differentiation of MOMCs into mesenchymal and endothelial lineages [9,12]. MOMCs cultured for 7 days under a mesenchymal-induction condition, as described previously [9], were analyzed for mesenchymal lineage-specific transcription factors, such as Cbfa1 for osteogenesis, Sox-9 for chondrogenesis, and peroxisome proliferation-activated receptor γ (PPARγ) for adipogenesis. For these analyses, the cells were incubated with goat anti-Cbfa1 or anti-Sox-9 polyclonal antibodies, or mouse anti-PPARγ mAb (Santa Cruz Biotechnology, Santa Cruz, CA), followed by AlexaFluor® 568 anti-goat or -mouse IgG antibodies (Molecular Probes, Eugene, OR). The cells were incubated with FITC-conjugated mouse anti-CD45 mAb (Dako Carpinteria, CA) and observed under a fluorescence microscope (IX82; Olympus, Tokyo, Japan).

In some experiments, mesenchymal induction cultures were maintained for 3 to 4 weeks, and differentiation into functional osteoblasts, chondroblasts, and adipocytes was detected by alizarin red staining, immunostaining for type II collagen, and oil red O staining, respectively [9]. The differentiation of MOMCs into the endothelial lineage was evaluated by fluorescent staining with mouse anti-endothelial nitric oxide synthase (eNOS) mAb (BD Biosciences) or rabbit anti-Tie-2 polyclonal antibodies (Santa Cruz Biotechnology), followed by incubation with AlexaFluor® 568 anti-mouse or anti-rabbit IgG antibodies (Molecular Probes) [12]. Negative controls were slides incubated with isotype-matched mouse or rabbit mAb to an irrelevant antigen, instead of the primary antibody. Nuclei were counter-stained with 4′, 6-diamidino-2-phenylindole, dihydrochloride (DAPI).

Statistical Analysis

All continuous values are shown as the mean ± standard deviation (SD). Comparisons between two groups were tested for statistical significance using the non-parametric Mann-Whitney *U* test.

Results

Identification of Circulating $CD14^-$ cells Required For Generating MOMCs

We previously reported that to generate MOMCs, circulating $CD14^+$ monocytes are required to bind to fibronectin and be exposed to peripheral blood $CD14^-$ cells [9]. To identify the circulating $CD14^-$ cells required for generating MOMCs, we first evaluated the potential role of platelets that contaminated the PBMC fraction isolated by Lymphoprep density-gradient centrifugation. We prepared $CD14^+$ monocytes and $CD14^-$ PBMCs from the PBMC fraction after removing the contaminating platelets by negative selection with anti-CD61 mAb-coupled

magnetic beads. In addition, circulating platelets were isolated using a gel-filtration method to avoid activating the platelets during the separation procedure. Next, we set up MOMC generation cultures in which $CD14^+$ monocytes were cultured alone, with platelets, or with platelet-depleted $CD14^-$ PBMCs on fibronectin-coated plastic plates. More adherent cells appeared in the cultures with platelets or $CD14^-$ PBMCs than in the culture with monocytes alone (Figure 1A and B). Adherent cells with a fibroblastic morphology typical of MOMCs predominated in the cultures with monocytes and platelets, but were rarely detected in those with monocytes alone or with monocytes and $CD14^-$ PBMCs. Flow cytometric analysis showed that CD34 was expressed by the adherent $CD14^+$ cells obtained from the cultures of monocytes and platelets, but not by those from cultures of monocytes alone or monocytes with $CD14^-$ PBMCs (Figure 1C).

The adherent cells obtained in these cultures were placed in differentiation induction cultures to assess their ability to differentiate into mesenchymal and endothelial lineages. As shown in Figure 1D, the adherent cells obtained in cultures with monocytes and platelets showed nuclear expression of the lineage-specific transcription factors Cbfa1, Sox-9, and PPARγ together with CD45, upon 7-day osteogenic, chondrogenic, and adipogenic induction treatment, respectively, and expression of the endothelial markers eNOS and Tie-2 upon endothelial induction treatment. In addition, functional osteoblasts, chondrocytes, and adipocytes were detected after 3 weeks of osteogenic, chondrogenic, and adipogenic induction treatment of adherent cells obtained in cultures with monocytes and platelets (data not shown). Adherent cells obtained in cultures of monocytes alone or monocytes plus $CD14^-$ PBMCs lacked the capacity to differentiate into mesenchymal or endothelial lineages. Concordant findings were obtained from peripheral blood cells derived from three additional donors. Adherent cells obtained in cultures of monocytes and platelets on fibronectin had typical MOMC characteristics, including fibroblast-like morphology, CD34 expression, and the potential to differentiate toward mesenchymal and endothelial lineages [9], indicating that platelets are the primary circulating cell population contributing to the transformation of circulating $CD14^+$ monocytes into MOMCs.

We next examined whether platelet-conditioned medium could be substituted for whole platelets for generating MOMCs. For this purpose, we evaluated MOMC generation by culturing $CD14^+$ monocytes with platelets, or with platelet-conditioned medium prepared by culturing platelets on fibronectin. These two cultures yielded adherent cells with fibroblastic morphology with almost the same efficiency (Figure 2A and B). Flow cytometry showed similar scatter distributions and CD34 expression in the adherent cells obtained in these cultures (Figure 2C). The adherent cells obtained in these cultures were able to differentiate into mesenchymal and endothelial lineages according to the induction treatment (data not shown). Thus, MOMCs could be generated in the presence of soluble factors released by platelets that have been activated by exposure to fibronectin.

We further evaluated the MOMC-generation capacity of platelet-conditioned media prepared by stimulation with a variety of platelet agonists, including thrombin, thrombin receptor activation peptide, type I collagen, ADP, ristocetin, and epinephrine. All the platelet agonists induced the release of MOMC-induction factor(s), which promoted the generation of MOMCs in cultures of $CD14^+$ monocytes on fibronectin. The representative morphology and flow cytometry analysis of CD34 expression in the adherent cells obtained in cultures containing platelet-conditioned medium prepared by stimulation with thrombin or ADP are shown in Figure 2D. Consistent results were obtained from independent experiments using peripheral blood cells from three additional donors. These results indicated that, to generate MOMCs, circulating $CD14^+$ monocytes are required to be exposed to soluble factor(s) released from activated platelets, irrespective of the agonistic stimulation.

Screening and Identification of a MOMC Differentiation Factor

To screen for MOMC differentiation factor(s), the capacity to transform $CD14^+$ monocytes into MOMCs was evaluated by the appearance of adherent cells with fibroblast-like morphology and CD34 expression, observed by flow cytometry, and the ability to differentiate into various lineages. $CD14^+$ monocytes were cultured with fibronectin in the presence of thrombin-stimulated platelet-conditioned media fractionated based on a protein MW greater or smaller than 30 kDa (Figure 3). The capacity to generate MOMCs was retained in the platelet-condition medium enriched for proteins with a MW <30 kDa. Concordant results were obtained from five donors.

We then selected 16 candidate soluble factors required for MOMC generation, based on (i) being released from platelets upon activation and (ii) having a MW <30 kDa. These candidate factors included IL-7, EGF, bFGF, TGF-β, PDGF-AA, PDGF-AB, IL-8, GRO-α, ENA78, TARC, SDF-1, PF4, RANTES, MIP-1α, MCP-3, and NAP2. Serial concentrations of these candidate cytokines, growth factors, and chemokines were added to cultures of $CD14^+$ monocytes on fibronectin derived from five donors, and the generation of MOMCs was evaluated (Figure 4). SDF-1 and RANTES were selected as potent factors that promoted the generation of spindle-like adherent cells in a dose-dependent manner ($P<0.05$ for both comparisons); bFGF, MIP-1α, and MCP-3 also promoted the appearance of adherent cells to some extent. Among the adherent cells generated in cultures with these candidate soluble factors, CD34 expression was detected in the monocytes cultured with SDF-1, but not in those cultured with RANTES, bFGF, MIP-1α, or MCP-3.

To confirm that SDF-1 was capable of inducing MOMCs, $CD14^+$ monocytes from 10 independent donors were cultured on fibronectin in the presence of serial concentrations of SDF-1. SDF-1 increased the number of adherent cells with fibroblast-like morphology, in a dose-dependent manner (Figure 5A and B). Adherent cells generated in the presence of SDF-1 expressed CD34 (Figure 5C) and had multidifferentiation potential toward the osteogenic, chondrogenic, adipogenic, and endothelial lineages (Figure 5D). In addition, functional osteoblasts, chondrocytes, and adipocytes were successfully generated with 4-week mesenchymal induction treatment (data not shown). SDF-1 is a chemotactic factor for a variety of hematopoietic-lineage cells expressing the SDF-1 receptor CXCR4. To examine how blocking the interaction between SDF-1 and CXCR4 would affect MOMC generation, monocyte cultures on fibronectin with thrombin-treated platelet-conditioned medium were prepared in the presence of serial concentrations of AMD 3100, a CXCR4 antagonist. As shown in Figure 5E, AMD 3100 suppressed the generation of spindle-shaped adherent cells in a dose-dependent fashion.

These findings together indicate that the platelet-derived factor SDF-1 is required for generating MOMCs. However, in MOMC generation cultures consisting of $CD14^+$ monocytes, fibronectin, and SDF-1, at least 5% FBS was required in the media to generate MOMCs (results not shown), indicating that other factor(s) in the serum were also required.

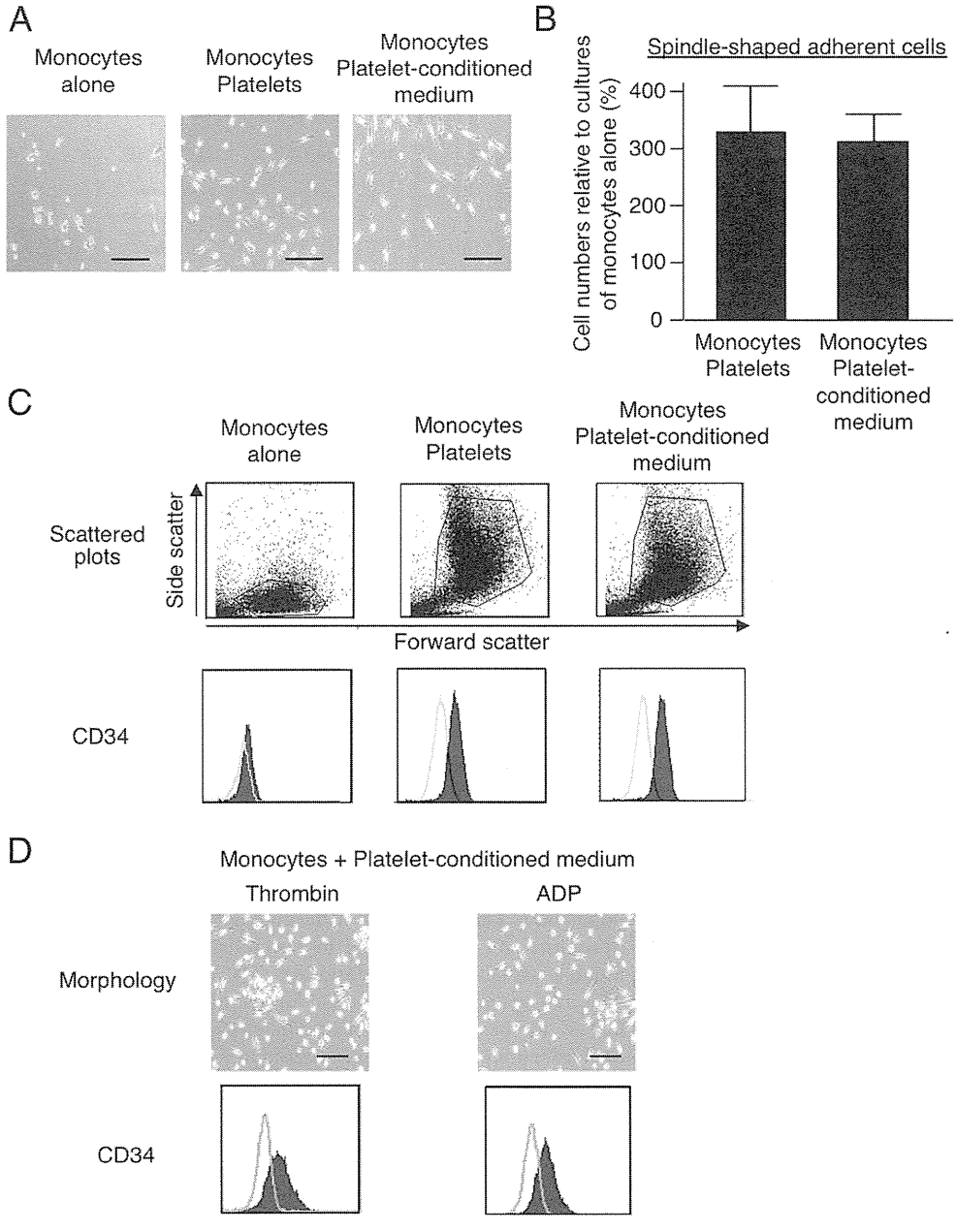

Figure 2. Soluble factor(s) released from activated platelets are required for MOMC generation. $CD14^+$ monocytes were cultured alone or in combination with platelets or platelet-conditioned medium on fibronectin. (**A**) Morphology of adherent cells on culture day 7. Bars: 200 μm. (**B**) Spindle-shaped adherent cells generated in the indicated culture, expressed as a proportion (%) of those generated in a culture of monocytes alone. Results show the mean and SD of three independent experiments. (**C**) Scatter plots and surface expression of CD34 on adherent cells, analyzed by flow cytometry. CD34 expression is shown by a closed histogram; open histograms represent staining with isotype-matched control mAb. (**D**) The morphology and CD34 expression of adherent cells obtained from cultures with platelet-conditioned medium prepared by stimulating platelets with thrombin or ADP. Bars: 200 μm. Cell-surface CD34 expression, analyzed by flow cytometry, is shown by closed histograms.
doi:10.1371/journal.pone.0074246.g002

Effect of the Circulating $CD14^+$ Monocytes' CXCR4 Expression Level on the MOMC Differentiation Capacity

Nearly all the $CD14^+$ monocytes in circulation express CXCR4 on their surface, but the expression level is highly variable (Figure 6A). The expression level of CXCR4 was almost the same between $CD14^+$ monocytes derived from peripheral blood samples anticoagulated with heparin and sodium citrate. To evaluate how the level of CXCR4 expressed by circulating $CD14^+$ monocytes affects their capacity to differentiate into MOMCs, we prepared $CXCR4^{high}$ and $CXCR4^{low}$ monocytes using fluorescent-activated cell sorting (Figure 6B). Flow cytometry revealed that these two cell populations expressed CXCR4 differently. The $CD14^+CXCR4^{high}$ and $CD14^+CXCR4^{low}$ cells were then cultured on fibronectin in the presence of thrombin-treated platelet-condition medium. Since nearly all the $CD14^+$ monocytes in circulation express CD11a, $CD14^+CD11a^+$ cells prepared by fluorescent-activated cell sorting were used as a control. After 7 days of culture, spindle-shaped adherent cells appeared more

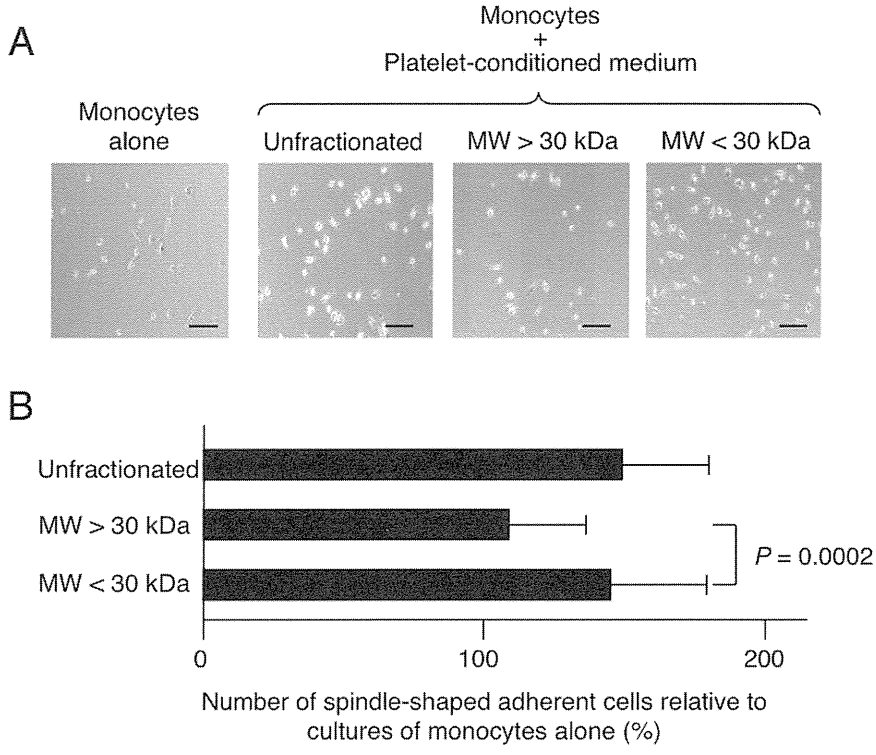

Figure 3. The MOMC generation activity resides in the MW <30-kDa fraction of platelet-conditioned medium. $CD14^+$ monocytes were cultured on fibronectin with or without unfractionated or fractionated platelet-conditioned medium prepared by stimulating platelets with thrombin. (**A**) Adherent cell morphology on culture day 7. Bars: 200 μm. (**B**) The generation of spindle-shaped adherent cells in the indicated cultures, expressed as a proportion (%) of those generated by culturing monocytes alone. Results show the mean and SD of three independent experiments.
doi:10.1371/journal.pone.0074246.g003

frequently in cultures of $CD14^+CXCR4^{high}$ cells than in cultures of $CD14^+CXCR4^{low}$ cells (Figure 6C and D), although adherent cells from these cultures expressed CD34 similarly (data not shown). Adherent cells obtained from the $CD14^+CXCR4^{high}$ cell cultures expressed Cbfa1, Sox-9, and PPARγ upon 7-day osteogenic, chondrogenic, and adipogenic induction cultures, respectively, and expressed eNOS and Tie-2 in endothelial induction cultures (Figure 6E). In contrast, these lineage-specific transcription factors and endothelial proteins were scarcely detectable in the adherent cells cultured from $CD14^+CXCR4^{low}$ cells. MOMCs were also generated by culturing $CD14^+CXCR4^{high}$ cells in the presence of SDF-1 instead of platelet-conditioned medium (data not shown). These results together indicate that MOMC precursors are abundant in the circulating $CD14^+CXCR4^{high}$ cell fraction.

Discussion

Using a stepwise approach, this study successfully identified SDF-1 as a soluble factor required for transforming circulating $CD14^+$ monocytes into MOMCs. First, we found that platelets played a critical role in generating MOMCs from circulating $CD14^+$ monocytes. Subsequently, soluble factors with a MW <30 kDa released from activated platelets were shown to contain MOMC differentiation factor(s). The screening of candidate platelet-derived soluble factors identified SDF-1 as a factor required for MOMC generation. The critical role of SDF-1 in this process was further confirmed by the finding that blocking the SDF-1-CXCR4 interaction with AMD 3100 inhibited the MOMC generation. Finally, we found that circulating monocytic MOMC precursors were enriched in the $CD14^+CXCR4^{high}$ cell population. Taken together with our previous findings [15], the transformation of circulating monocytes into MOMCs requires multiple signals through cell-surface $\alpha_5\beta_1$ integrin and CXCR4. This information should be useful for investigating how circulating $CD14^+$ monocytes acquire multidifferentiation potential, and for establishing an optimal culture condition for generating MOMCs for potential use in regenerative medicine.

SDF-1, also designated CXCL12, is a chemotactic factor for such varied cell types as stem cells, progenitor cells, and mature hematopoietic-lineage cells, such as monocytes. During embryogenesis, SDF-1 is critically involved in the development of hematopoietic, nerve, and endothelial tissues through its regulation of tissue progenitor cell migration, homing, and survival [17,18]. In adult life, the SDF-1-CXCR4 axis is the key factor for stem- and immune-cell trafficking. For example, hematopoietic stem cells migrate from the bone marrow along the SDF-1 concentration gradient and contribute to tissue repair [19,20]. Moreover, Yamaguchi and colleagues found that SDF-1 released from activated platelets into the microcirculation is functionally involved in recruiting bone marrow-derived endothelial progenitor cells to vascular injury areas [21]. In contrast to its chemotactic activities, we have found that SDF-1 also modulates the cellular phenotype and differentiation potential of circulating $CD14^+$ monocytes.

Although relatively little is known about CXCR4′ s downstream signaling cascades, it has been shown that the binding of SDF-1 to CXCR4 in hematopoietic-lineage cells triggers G protein-mediated downstream signaling, including phosphoinositide-3 kinase, protein kinase A, protein kinase C, and mitogen-activated protein kinase, as well as G protein-independent tyrosine phosphorylation

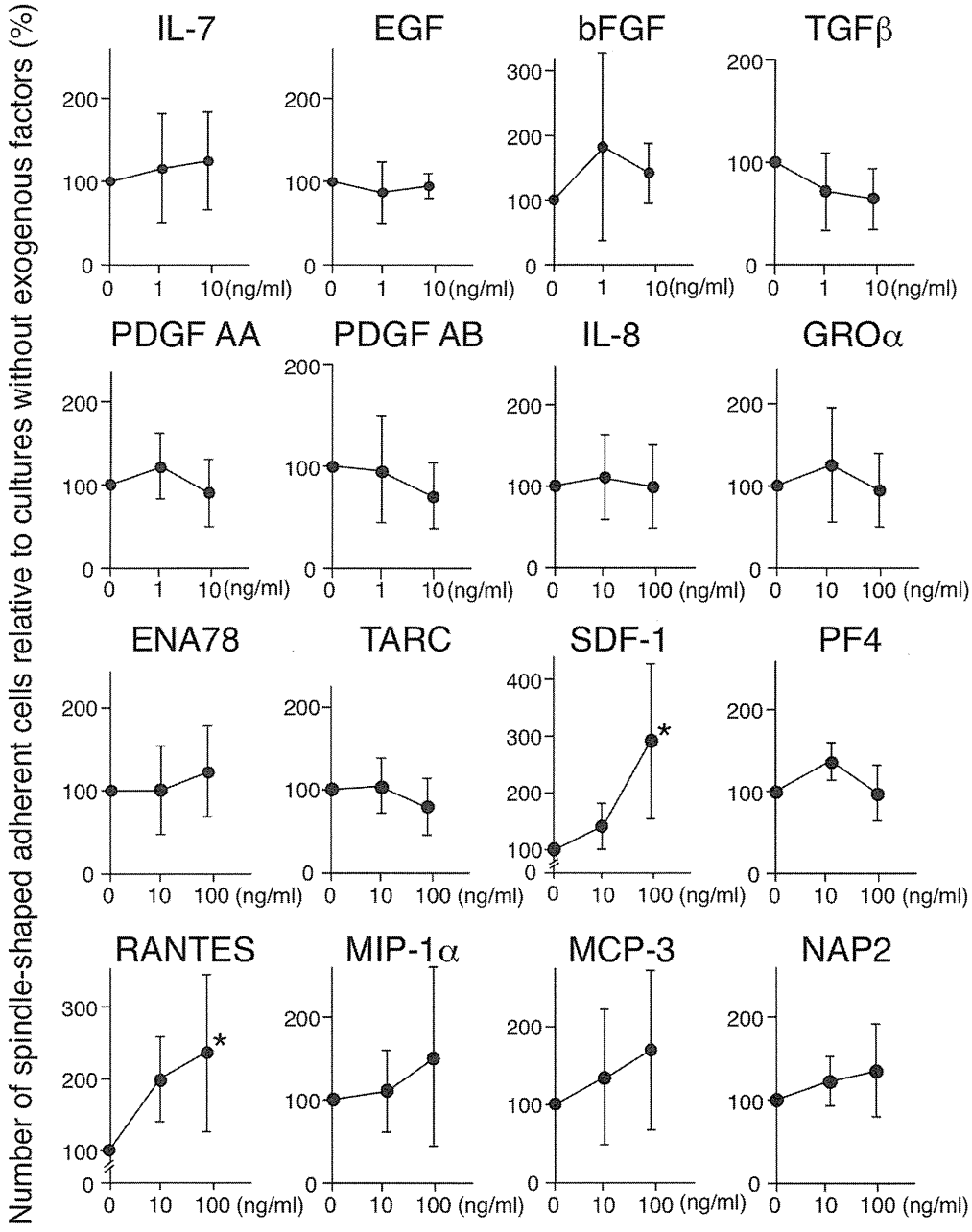

Figure 4. Screening of MOMC differentiation factor(s): 16 candidate cytokines, growth factors, and chemokines. $CD14^+$ monocytes were cultured on fibronectin with or without serial concentrations of various soluble factors released by activated platelets and having a MW <30 kDa. The generation of spindle-shaped adherent cells was expressed as a proportion (%) of those generated by culturing monocytes alone. Results show the mean and SD of five independent experiments. *$P<0.05$, compared with the culture without exogenous factors. IL, interleukin; EGF, epidermal growth factor; bFGF, basic fibroblast growth factor; TGFβ, transforming growth factor-β; PDGF, platelet-derived growth factor; GROα, growth-related oncogene-α; ENA78, epithelial cell-derived neutrophil-activating peptide 78; TARC, thymus and activation-regulated chemokine; SDF-1, stromal cell-derived factor-1; PF4, platelet factor 4; RANTES, regulated upon activation, normal T cell expressed and secreted; MIP-1α, macrophage inflammatory protein-1α; MCP-3, monocyte chemotactic protein-3; and NAP2, neutrophil-activating peptide 2.
doi:10.1371/journal.pone.0074246.g004

of Janus kinase (JAK) 2 and other members of the JAK signal transduction pathway [22]. These effector pathways regulate cell adhesion, locomotion, and chemotaxis, but how these signaling pathways elicit biological effects, such as proliferation and differentiation, is controversial. Given that $\alpha_5\beta_1$ integrin is also required for generating MOMC [15], interactions between CXCR4 and integrin signals are of potential interest [23]. In this regard, it has been reported that CXCR4 and integrin signals interact with each other and are crucial for retaining progenitor cells in the bone marrow by phosphorylating c-kit [24], a receptor tyrosine kinase that functions in such diverse biological functions as proliferation, survival, and differentiation [25]. To determine the mechanisms underlying the transdifferentiation of circulating monocytes into multipotential cells, we must examine the downstream signaling pathways of CXCR4 and $\alpha_5\beta_1$ integrin.

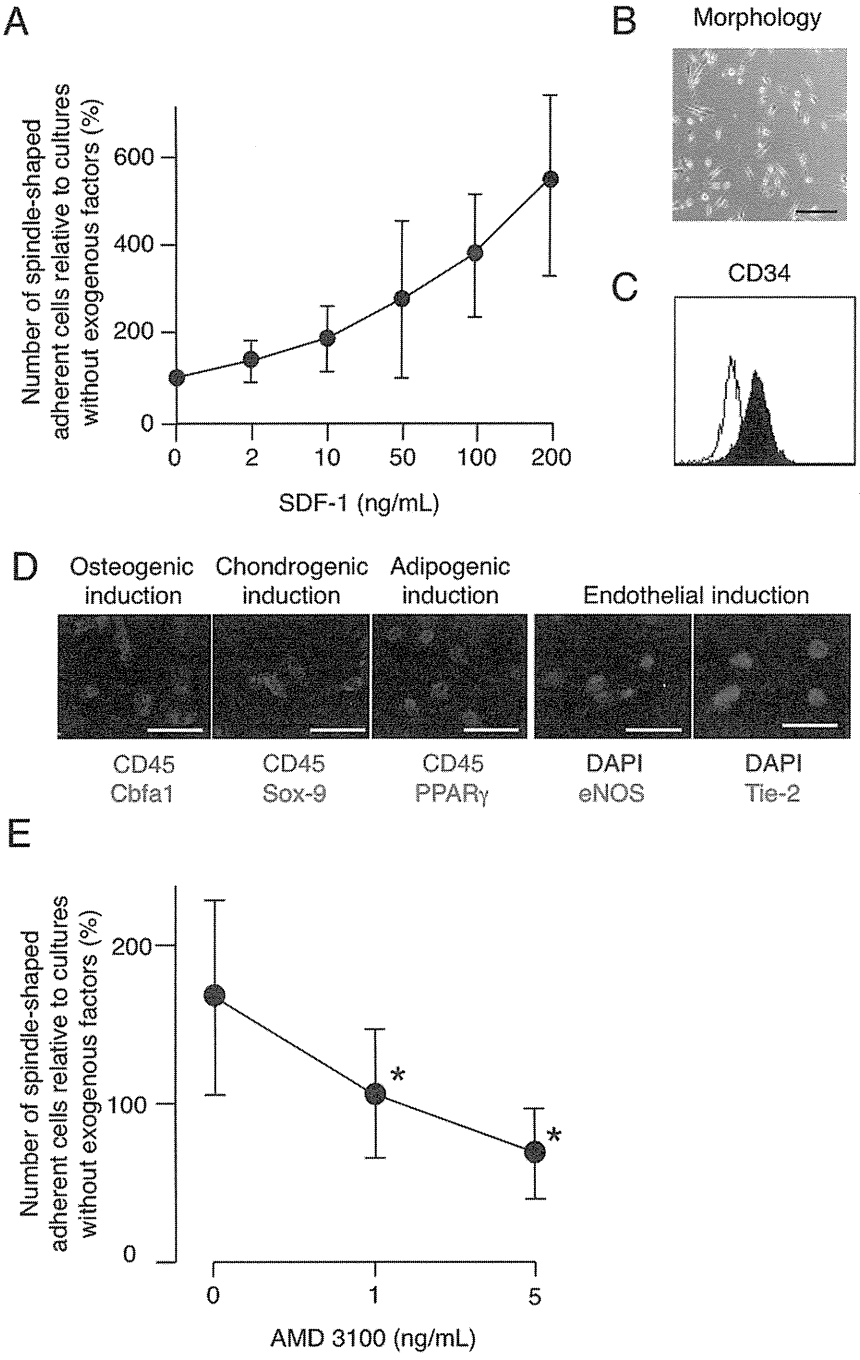

Figure 5. SDF-1 is required for generating MOMCs. $CD14^+$ monocytes were cultured on fibronectin in the presence of serial concentrations of SDF-1. (**A**) The generation of spindle-shaped adherent cells, expressed as a proportion (%) of those generated from culturing monocytes alone. The results shown are the mean and SD of 10 independent experiments. (**B**) Morphology of adherent cells obtained in a culture with 100 ng/ml SDF-1. Bars: 200 μm. (**C**) Cell-surface CD34 expressed on adherent cells obtained in a culture with 100 ng/ml SDF-1, as analyzed by flow cytometry. Closed histograms indicate CD34 expression; open histograms represent staining with isotype-matched control mAb. (**D**) Multidifferentiation potential of adherent cells obtained in a culture with 100 ng/ml SDF-1. Cells treated for osteogenic, chondrogenic, adipogenic, and endothelial induction for 1 week were analyzed by immunohistochemical staining for Cbfa1, Sox-9, or PPARγ (red) in combination with CD45 (green), or for eNOS or Tie-2 (red) in combination with DAPI (blue), and were observed under a fluorescence microscope. Representative results of 3 independent experiments are shown. Bars: 50 μm. (**E**) AMD 3100, a CXCR4 antagonist, suppressed the generation of MOMCs. Circulating monocytes were cultured with platelet-conditioned medium on fibronectin in the presence of 0, 1, or 5 ng/ml AMD 3100. Results are expressed as a proportion (%) of the number of spindle-shaped adherent cells obtained in the culture of monocytes alone. *$P<0.05$, compared with culturing without AMD 3100.
doi:10.1371/journal.pone.0074246.g005

Activated platelets are known to release a variety of soluble factors stored in their granules, including cytokines, chemokines, and growth factors [16]. Interestingly, SDF-1 is produced mainly by mesenchymal cells and endothelium, not by platelets or other hematopoietic-lineage cells. Platelets hold substantial amounts of SDF-1 in their granules that exists in a complex with CXCR4, and

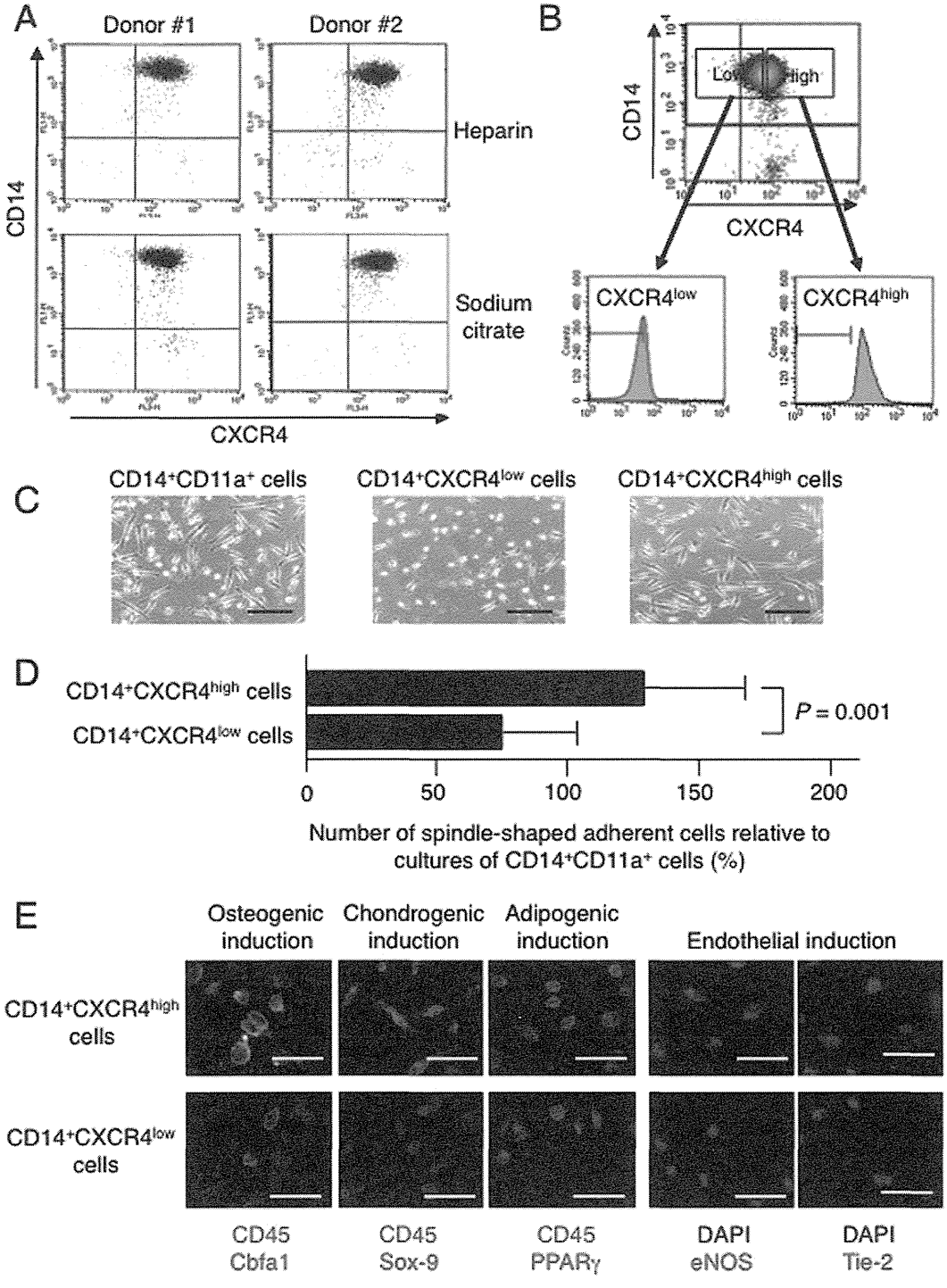

Figure 6. MOMC precursors are enriched in CD14$^+$CXCR4^{high} cells. (**A**) Dot-plot analysis of expression of CD14 and CXCR4 in CD14$^+$ monocytes derived from 2 independent donors. Peripheral blood samples were anticoagulated with heparin or sodium citrate immediately after blood sampling. (**B**) Dot-plot analysis of CXCR4 expression in CD14$^+$ cells, gated by CXCR4^{high} and CXCR4^{low} cells for fluorescent-activated cell sorting. Cell-surface CXCR4 on CXCR4^{high} and CXCR4^{low} cells is shown as histograms. (**C**) Morphology of adherent cells obtained from CD14$^+$CD11a$^+$, CD14$^+$CXCR4^{high}, or CD14$^+$CXCR4^{low} cells cultured on fibronectin with platelet-conditioned medium. Bars: 200 μm. (**D**) The generation of spindle-shaped adherent cells, expressed as a proportion (%) of those generated by culturing CD14$^+$CD11a$^+$ cells. Results show the mean and SD of three independent experiments. (**F**) Multidifferentiation potential of cells obtained by culturing CD14$^+$CXCR4^{high} and CD14$^+$CXCR4^{low} cells. Cells treated for osteogenic, chondrogenic, adipogenic, and endothelial induction for 1 week were analyzed by immunohistochemical staining for Cbfa1, Sox-9, or PPARγ (red) in combination with CD45 (green), or for eNOS or Tie-2 (red) in combination with DAPI (blue), and were observed under a fluorescence microscope. Representative results of 3 independent experiments are shown. Bars: 50 μm.
doi:10.1371/journal.pone.0074246.g006

release SDF-1 when activated by various agonists [26]. Platelets have long been considered to function solely as chief effector cells in hemostasis. However, the growing evidence that soluble mediators released from activated platelets are involved not only in hemostasis, but also in inflammation, innate/adaptive immune responses, and tissue repair indicates that platelets are more multifunctional than previously thought [27].

Circulating monocytes are recruited to extra-vascular injury sites, where they are exposed to inflammatory cytokines, and differentiate into macrophages that take up debris, clean the tissue, and induce an acquired immune response. Since the differentiation of $CD14^{+}CXCR4^{high}$ monocytic precursors into MOMCs requires that the monocytes bind to fibronectin and be exposed to SDF-1 released from activated platelets, circulating monocytes may encounter these signals at the injury site. In that case, these external signals would induce specific intracellular signals in the infiltrating monocytic precursors, leading to the acquisition of mesenchymal and endothelial differentiation potentials. The MOMCs would subsequently differentiate into tissue-specific cells in response to organ-specific environmental cues.

Fibrocytes, a population of circulating cells with fibroblast properties, are characterized by a distinctive phenotype positive for CD45, CD34, and type I collagen [28]. MOMCs and fibrocytes in cultures commonly have spindle-shaped morphology and express CD34 and type I collagen, but have several distinct characteristics. Specifically, MOMCs are generated from circulating $CD14^{+}$ monocytes without expression of CD34 [9]: this phenotypic feature is apparently distinct from that of circulating fibrocytes ($CD45^{+}CD34^{+}$type I collagen^{+}). In addition, fibrocytes are able to self-replicate and expand in long-term cultures [28], whereas MOMCs have limited lifespan at least *in vitro* [8,9]. Finally, isolation of fibrocytes in PBMC cultures requires either fibronectin or type I collagen [26], but MOMC induction cultures using type I collagen instead of fibronectin fail to generate $CD34^{+}$ cells with multiple differentiation potentials [15]. These findings strongly suggest that circulating MOMC precursors are different from fibrocytes.

In summary, our results indicate that MOMCs are generated from circulating $CD14^{+}CXCR4^{high}$ monocytic precursors through their exposure to fibronectin and SDF-1. These findings are helpful for understanding the mechanisms at work in the transdifferentiation of monocytic progenitors into multipotential cells, and the role of these cells in physiologic and pathogenic states.

Author Contributions

Conceived and designed the experiments: HM TK MK. Performed the experiments: NS YO MK. Analyzed the data: NS YO HM TK MK. Contributed reagents/materials/analysis tools: MK. Wrote the paper: NS MK.

References

1. Godon S (1995) The macrophage. Bioessays 17: 977–986.
2. Miyamoto T, Ohneda O, Arai F, Iwamoto K, Okada S, et al. (2001) Bifurcation of osteoclasts and dendritic cells from common progenitors. Blood 98: 2544–2554.
3. Servet-Delprat C, Arnaud S, Jurdic P, Nataf S, Grasset MF, et al. (2002) $Flt3^{+}$ macrophage precursors commit sequentially to osteoclasts, dendritic cells and microglia. BMC Immunol 3: 15–25.
4. Zhao Y, Glesne D, Huberman E (2003) A human peripheral blood monocyte-derived subset acts as pluripotent stem cells. Proc Natl Acad Sci USA 100: 2426–2431.
5. Romagnani P, Annunziato F, Liotta F, Lazzeri E, Mazzinghi B, et al. (2005) $CD14^{+}CD34^{low}$ cells with stem cell phenotypic and functional features are the major source of circulating endothelial progenitors. Circ Res 97: 314–322.
6. Bucala R, Spiegel LA, Chesney J, Hogan M, Cerami A (1994) Circulating fibrocytes define a new leukocyte subpopulation that mediates tissue repair. Mol Med 1: 71–81.
7. Seta N, Kuwana M (2007) Human circulating monocytes as multipotential progenitors. Keio J Med 56: 41–47.
8. Seta N, Kuwana M (2010) Derivation of multipotent progenitors from human circulating $CD14^{+}$ monocytes. Exp Hematol 38: 556–583.
9. Kuwana M, Okazaki Y, Kodama H, Izumi K, Yasuoka H, et al. (2003) Human circulating $CD14^{+}$ monocytes as a source of progenitors that exhibit mesenchymal cell differentiation. J Leukoc Biol 74: 833–845.
10. Kodama H, Inoue T, Watanabe R, Yasuoka H, Kawakami Y, et al. (2005) Cardiomyogenic potential of mesenchymal progenitors derived from human circulating $CD14^{+}$ monocytes. Stem Cell Dev14: 676–686.
11. Kodama H, Inoue T, Watanabe R, Yasutomi D, Kawakami Y, et al. (2006) Neurogenic potential of progenitors derived from human circulating $CD14^{+}$ monocytes. Immunol Cell Biol 84: 209–217.
12. Kuwana M, Okazaki Y, Kodama H, Satoh T, Kawakami Y, et al. (2006) Endothelial differentiation potential of human monocyte-derived multipotential cells. Stem Cells 24: 2733–2743.
13. Hattori H, Suzuki S, Okazaki Y, Suzuki N, Kuwana M (2012) Intracranial transplantation of monocyte-derived multipotential cells enhances recovery after ischemic stroke in rats. J Neurosci Res 90: 479–488.
14. Yamaguchi Y, Okazaki Y, Seta N, Satoh T, Takahashi K, et al. (2010) Enhanced angiogenic potency of monocytic endothelial progenitor cells in patients with systemic sclerosis. Arthritis Res Ther 12: R205.
15. Seta N, Okazaki Y, Izumi K, Miyazaki H, Kato T, et al. (2012) Fibronectin binding is required for acquisition of mesenchymal/endothelial differentiation potential in human circulating monocytes. Clin Dev Immunol 2012: 820827.
16. Walkowiak B, Kralisz U, Michalec L, Majewska E, Koziolkiewicz W, et al. (2000) Comparison of platelet aggregability and P-selectin surface expression on platelets isolated by different methods. Thromb Res 99: 495–502.
17. Nagasawa T, Hirota S, Tachibana K, Takakura N, Nishikawa S, et al. (1996) Defects of B-cell lymphopoiesis and bone-marrow myelopoiesis in mice lacking the CXC chemokine PBSF/SDF-1. Nature 382: 635–638.
18. Zou YR, Kottmann AH, Kuroda M, Taniuchi I, Littman DR (1998) Function of the chemokine receptor CXCR4 in haematopoiesis and in cerebellar development. Nature 393: 595–599.
19. Massberg S, Konrad I, Schürzinger K, Lorenz M, Schneider S, et al. (2006) Platelets secrete stromal cell-derived factor 1alpha and recruit bone marrow-derived progenitor cells to arterial thrombi in vivo. J Exp Med 203: 1221–1233.
20. Kucia M, Ratajczak J, Reca R, Janowska-Wieczorek A, Ratajczak MZ (2004) Tissue-specific muscle, neural and liver stem/progenitor cells reside in the bone marrow, respond to an SDF-1 gradient and are mobilized into peripheral blood during stress and tissue injury. Blood Cells Mol Dis 32: 52–57.
21. Hattori K, Heissig B, Tashiro K, Honjo T, Tateno M, et al. (2001) Plasma elevation of stromal cell-derived factor-1 induces mobilization of mature and immature hematopoietic progenitor and stem cells. Blood 97: 3354–3360.
22. Sharma M, Afrin F, Satija N, Tripathi RP, Gangenahalli GU (2011) Stromal-derived factor-1/CXCR4 signaling: indispensable role in homing and engraftment of hematopoietic stem cells in bone marrow. Stem Cells Dev 20: 933–946.
23. Peled A, Kollet O, Ponomaryov T, Petit I, Franitza S, et al. (2000) The chemokine SDF-1 activates the integrins LFA-1, VLA-4, and VLA-5 on immature human $CD34^{+}$ cells: role in transendothelial/stromal migration and engraftment of NOD/SCID mice. Blood 95: 3289–3296.
24. Cheng M, Qin G (2012) Progenitor cell mobilization and recruitment: SDF-1, CXCR4, α4-integrin, and c-kit. Prog Mol Biol Transl Sci 111: 243–264.
25. Edling CE, Hallberg B (2007) c-Kit-a hematopoietic cell essential receptor tyrosine kinase. Int J Biochem Cell Biol 39: 1995–1998.
26. Vieira-de-Abreu A, Campbell RA, Weyrich AS, Zimmerman GA (2011) Platelets: versatile effector cells in hemostasis, inflammation, and the immune continuum. Semin Immunopathol 34: 5–30.
27. Weyrich AS, Zimmerman GA (2004) Platelets: signaling cells in the immune continuum. Trends Immunol 25: 489–495.
28. Bucala R, Spiegel LA, Chesney J, Hogan M Cerami A (1994) Circulating fibrocytes define a new leukocyte subpopulation that mediates tissue repair. Mol Med 1: 71–81.

Presence of desaturated hemoglobin enhances the contribution of blood cells to flow-mediated dilation in subjects with systemic sclerosis

Eisuke Amiya [a,1], Munenori Takata [a,1], Masafumi Watanabe [a,*], Takehiro Takahashi [b], Yoshihide Asano [b], Masaru Hatano [a], Atsuko Ozeki [a], Aya Watanabe [a], Shuichi Kawarasaki [a], Zenshiro Tamaki [b], Takashi Taniguchi [b], Yohei Ichimura [b], Tetsuo Toyama [b], Ryozo Nagai [c], Shinichi Sato [b], Issei Komuro [a,d]

[a] Department of Cardiovascular Medicine, Graduate School of Medicine, The University of Tokyo, Japan
[b] Department of Dermatology, Graduate School of Medicine, The University of Tokyo, Japan
[c] Jichi Medical School, Japan
[d] Department of Cardiovascular Medicine, Osaka University Graduate School of Medicine, Japan

ARTICLE INFO

Article history:
Received 31 March 2013
Accepted 6 April 2013
Available online 4 May 2013

Keywords:
Flow-mediated dilation
Hemoglobin
Desaturation
Systemic sclerosis

Systemic sclerosis (SSc) is characterized by alterations of the microvasculature, disturbances of the immune system, and massive deposition of collagen and other matrix substances in connective tissue. Endothelium is the target tissue of the pathological process of SSc, and the vasculature modified by the impairment of endothelial cell function affects the pathological process of SSc. SSc is also accompanied by respiratory dysfunction caused by interstitial lung disease, and subjects with SSc are likely to be exposed to hypoxic conditions.

In an experimental model, deoxygenation enhanced the interrelationship between platelets, nitric oxide (NO), and erythrocytes [1,2]. However, the impact of desaturated hemoglobin (Hb) on vascular function has not been clearly elucidated in the clinical setting.

In this study, we assessed the association between desaturation of Hb and flow-mediated dilation (FMD) response in subjects with SSc.

We studied 48 (26 diffuse-type and 22 limited-type) SSc and 23 control subjects. Endothelial function was assessed by FMD. FMD measurement was performed by amplitude and brightness mode ultrasonography using a linear-array 10-MHz transducer (UNEXEF18G, UNEX, Nagoya), as previously described [3]. All components of a standard informed consent form were explained to each subject, and written informed consent was obtained from all subjects. The study protocol conformed to the Declaration of Helsinki and was reviewed and approved by the University of Tokyo Institutional Review Board. All values were expressed as mean ± standard deviation. Univariate and linear regression analyses were used to evaluate the association between clinical variables, and a p-value < 0.05 was considered significant.

Both FMD and brachial artery diameter (BAD) decreased in subjects with SSc (FMD: 5.62 ± 2.71% vs 7.33 ± 2.95%, $p = 0.012$; BAD: 3.36 ± 0.58 mm vs 3.69 ± 0.50 mm, $p = 0.016$). In subjects with SSc, BAD correlated with Hb, platelet count, and the Hb to platelet count ratio (Hb/Plt). Among these factors, Hb/Plt demonstrated the most significant correlation with BAD [Hb: $R = 0.34$ ($p = 0.018$); Plt: $R = -0.32$ ($p = 0.027$); Hb/Plt: $R = 0.42$ ($p = 0.0031$)]. In contrast, such correlative relationships between blood cell counts and BAD were not observed in control subjects.

We divided the subjects with SSc into two groups based on the desaturated Hb value (high, >0.3 g/dL and low <0.3 g/dL) calculated using the following formula: desaturated Hb = Hb × {100 − [arterial oxygen saturation measured by pulse oximeter (SpO2)] / 100} [4]. The desaturated Hb values ranged from 0 to 0.9 g/dL (mean: 0.32; standard deviation: 0.22; median: 0.294). Right ventricular systolic pressure, heart rate, and white blood cell count were significantly different between the two groups (Table 1), whereas no differences in FMD or basal BAD were observed. The interrelationship between FMD and blood cells was also significantly different between the two groups. FMD had a negative correlative relationship with Hb/Plt in subjects with high desaturated Hb [$R = -0.48$ ($p = 0.020$)], which was not observed in subjects with low desaturated Hb [$R = 0.20$ ($p = 0.30$); Fig. 1a]. A comparison of the correlation coefficients between FMD and Hb/Plt in these two groups showed that the Z score, calculated by Fisher r to z transformation, was 2.35 ($p = 0.0094$), suggesting a significant difference in the contribution of blood cells to FMD between groups with low and high desaturated Hb. In addition, hemodynamic parameters such as systolic blood pressure, estimated glomerular filtration rate, and BAD corresponded to the Hb/Plt value in subjects with high desaturated Hb, whereas in subjects with low desaturated Hb, no significant differences were observed in these hemodynamic parameters (Fig. 1b). These results also suggested the enhanced hemodynamic effect of blood cells in the presence of desaturated Hb.

Table 1
Baseline characteristics of subjects with high (>0.3 g/dL) and low (<0.3 g/dL) desaturated Hb.

	Desaturated Hb <0.3	Desaturated Hb >0.3	p value
N	25	23	
Age (years)	53.7 ± 14.3	55.5 ± 14.6	0.34
Body surface area (m^2)	1.44 ± 0.12	1.56 ± 0.21	0.013
Systolic BP (mmHg)	103.3 ± 16.0	104.0 ± 10.2	0.43
Diastolic BP (mmHg)	59.0 ± 7.4	57.6 ± 8.4	0.27
Heart rate (/min)	64.5 ± 10.4	78.3 ± 21.5	0.0031
Hemoglobin (g/dL)	12.2 ± 1.7	12.7 ± 2.0	0.14
White blood cell (1000/μL)	6.3 ± 2.6	8.2 ± 3.7	0.025
Platelet count (10,000/μL)	25.7 ± 7.0	25.4 ± 5.3	0.43
Hb/Plt	0.51 ± 0.15	0.53 ± 0.19	0.29
eGFR (ml/min/1.73 m^2)	83.2 ± 18.9	77.1 ± 22.9	0.16
CRP (mg/dL)	0.32 ± 0.66	0.55 ± 1.01	0.19
BNP (pg/mL)	48.0 ± 66.0	68.4 ± 60.3	0.20
Right ventricular systolic pressure (mmHg)	32.0 ± 7.6	38.6 ± 10.6	0.020
Vascular parameter			
Brachial artery diameter (mm)	3.32 ± 0.56	3.40 ± 0.62	0.31
FMD (%)	5.68 ± 2.64	5.54 ± 2.83	0.43

Abbreviations: BP, blood pressure; Hb/Plt, Hemoglobin/platelet count ratio, eGFR, estimated glomerular filtration ratio; CRP, C-reactive protein; BNP, brain natriuretic peptide; and FMD, flow-mediated dilation.

* Corresponding author at: Department of Cardiovascular Medicine, Graduate School of Medicine, The University of Tokyo, 7-3-1 Hongo, Bunkyo-ku, Tokyo 113-8655, Japan. Tel.: +81 3 3815 5411.
E-mail address: masafumi-tky@umin.net (M. Watanabe).
[1] Amiya E. and Takata M. equally contributed to this manuscript.

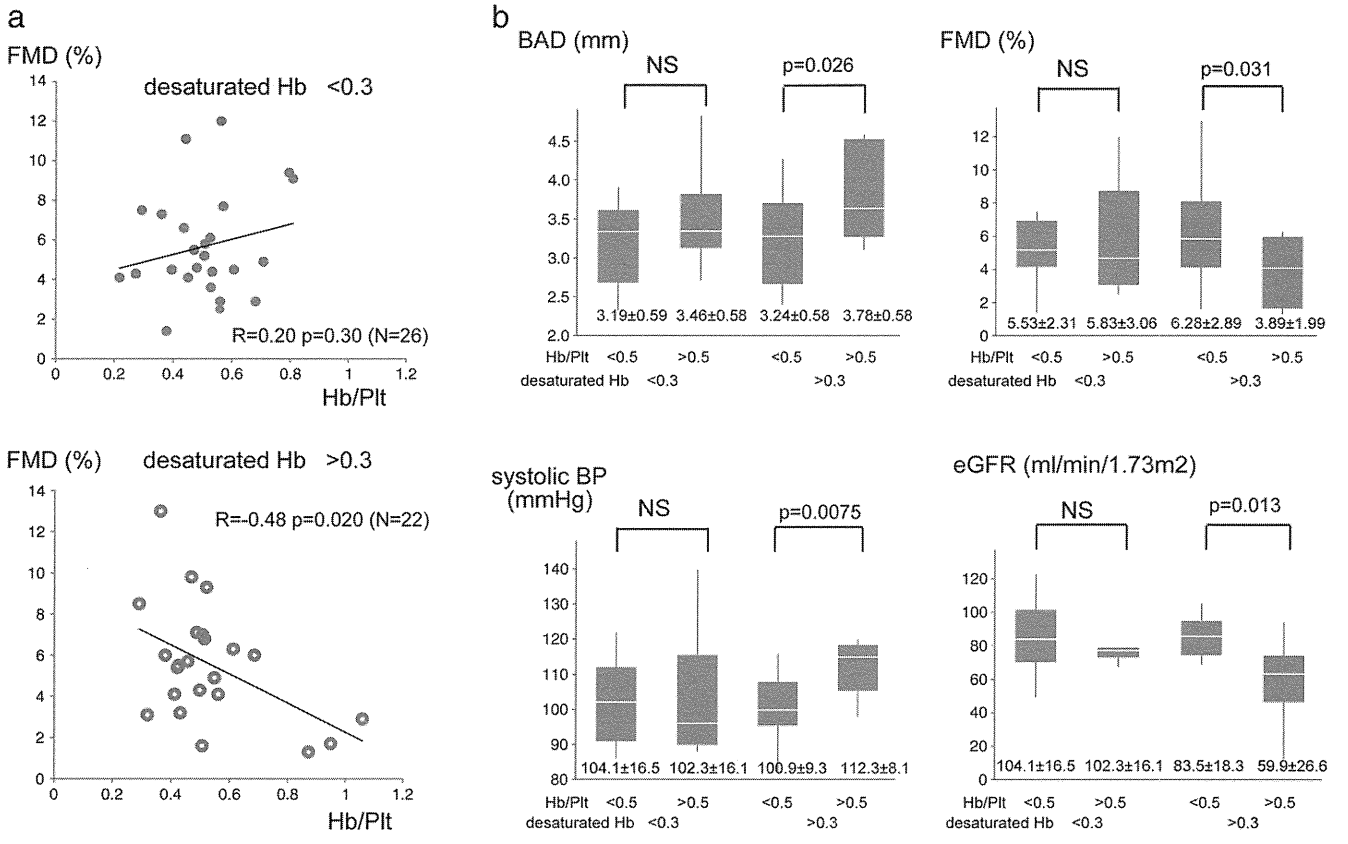

Fig. 1. a) Correlations between FMD and Hb/Plt in subjects with high (>0.3 g/dL) and low (<0.3 g/dL) desaturated Hb. Hb: hemoglobin, FMD: flow-mediated dilation, and Hb/Plt: hemoglobin to platelet count ratio. b) Differences of clinical variables between subjects with high (>0.5) and low (<0.5) hemoglobin to platelet count ratio (Hb/Plt) after subjects were divided into two groups, high (>0.3 g/dL) and low (<0.3 g/dL) desaturated Hb groups. The results are represented by box plots (middle hash of the box indicates the median; 25th–75th percentiles are represented by end caps of the box; whiskers extend to the last observed value) and presented in subjects with high and low desaturated Hb. BAD: brachial artery diameter, FMD: flow-mediated dilation, and eGFR: estimated glomerular filtration ratio.

This report provides a novel knowledge regarding the impact of blood cells on FMD response in the presence of desaturated Hb.

Hb regulates vascular dynamics through the following three pathways: S-nitrosohemoglobin-dependent bioactivity, adenosine 5′-triphosphate release, and deoxyhemoglobin-mediated regulation of NO [2]. Several studies have reported that increased Hb corresponds to the decline in FMD response in hypertensive or diabetic nephropathy subjects, suggesting that endothelial-derived vascular dilatation was greatly affected by the Hb value in the presence of vascular injury [5,6]. These reports suggested that vascular injury enhances the association between blood cells and vascular dynamics. In contrast, the present study suggests that the presence of desaturated Hb also increased the impact of blood cells on vascular dynamics. There are multiple complex pathways between NO metabolites and hemoglobin, and it is known that deoxygenated red blood cells lead to the reduction of nitrite to NO, leading to hypoxia-induced vasodilatation. However, the fate of NO derived from the endothelium in the presence of desaturated Hb is not yet clarified.

The baseline diameter and the association between the baseline diameter and blood cells were not different between groups with high and low desaturated Hb. Therefore, regulation of the baseline vascular diameter was not affected by the presence of desaturated Hb, whereas flow-mediated NO was influenced by its presence in a blood cell count-dependent manner.

Hb can scavenge NO produced by the endothelium, as demonstrated in cases of hemolysis in dialysis subjects in a clinical setting [7]. However, hemoglobin–NO reactions were significantly suppressed in the absence of hemolysis [8]. More rigorous experiments and studies are needed to elucidate the underlying mechanism. In addition, Hb/Plt, and not the absolute Hb value, most significantly correlated with FMD response in the present study. Platelets, which are another target of endothelium-derived NO, may regulate the accessibility or modulation of endothelium-derived NO to red blood cells.

The interrelationship between blood cells and vascular function should be clarified in each clinical situation when considering therapeutic strategies. In the present study, the contribution of Hb/Plt to FMD response was increased in the presence of desaturated Hb in subjects with vascular injury resulting from SSc. In the presence of desaturated Hb in subjects with SSc, FMD was more susceptible to blood cell effects, and the increase of Hb and decrease of platelet count led to the impairment of the magnitude of FMD, leading to a hemodynamic disadvantage.

References

[1] Srihirun S, Sriwantana T, Unchern S, et al. Platelet inhibition by nitrite is dependent on erythrocytes and deoxygenation. PLoS One 2012;7:e30380.
[2] Owusu BY, Stapley R, Patel RP. Nitric oxide formation versus scavenging: the red blood cell balancing act. J Physiol 2012;590:4993–5000.
[3] Watanabe S, Amiya E, Watanabe M, et al. Simultaneous heart rate variability monitoring enhances the predictive value of flow-mediated dilation in ischemic heart disease. Circ J 2012;77:1028-1025.
[4] Avidan A, Levin PD. Pulse oximetry. N Engl J Med 2011;365:184 [author reply 185].
[5] Natali A, Toschi E, Baldeweg S, et al. Haematocrit, type 2 diabetes, and endothelium-dependent vasodilatation of resistance vessels. Eur Heart J 2005;26:464–71.

[6] Sonmez A, Yilmaz MI, Saglam M, et al. The relationship between hemoglobin levels and endothelial functions in diabetes mellitus. Clin J Am Soc Nephrol 2010;5:45–50.
[7] Meyer C, Heiss C, Drexhage C, et al. Hemodialysis-induced release of hemoglobin limits nitric oxide bioavailability and impairs vascular function. J Am Coll Cardiol 2010;55:454–9.
[8] Azarov I, Liu C, Reynolds H, et al. Mechanisms of slower nitric oxide uptake by red blood cells and other hemoglobin-containing vesicles. J Biol Chem 2011;286:33567–79.

0167-5273/$ – see front matter
http://dx.doi.org/10.1016/j.ijcard.2013.04.046

Induced pluripotent stem cell models of long QT syndrome

Guoliang Li [a,b,c], Junqiang Pan [a,b,c,*], Aifeng Zhang [a,b,c,d], Chaofeng Sun [a,b,c,*]

[a] Department of Cardiology, First Affiliated Hospital of Xi'an Jiaotong University College of Medicine, No.277 Yanta West Road, Xi'an, Shaanxi 710061, P.R. China
[b] Institute of Cardiovascular Channelopathy, Key Laboratory of Environment and Genes Related to Diseases (Xi'an Jiaotong University), Ministry of Education, Xi'an, Shaanxi 710061, P.R. China
[c] Key Laboratory of Molecular Cardiology, Shannxi Province; No.277 Yanta West Road, Xi'an, Shaanxi 710061, P.R. China
[d] Department of Cardiology, Second Affiliated Hospital of Xi'an Jiaotong University College of Medicine, Xi'an, Shaanxi 710061, P.R. China

ARTICLE INFO

Article history:
Received 31 March 2013
Accepted 6 April 2013
Available online 7 May 2013

Keywords:
Induced pluripotent stem cells
Long QT syndrome
Toxicological testing
Drug screening
Cell therapies

Induced pluripotent stem cells (iPSCs), a type of pluripotent stem cell artificially derived from a non-pluripotent cell by inducing a "forced" expression of specific genes, have achieved great progress since it was firstly established [1]. iPSC technology provides a potential solution to overcome the drawbacks of conventional methods to model human diseases. Inherited long QT syndrome (LQTS) is an inborn heart condition, which predisposes patients to a potentially fatal ventricular arrhythmia. To date, hundreds of mutations in 13 different genes have been indentified to cause LQTS [2]. The pathophysiological feature of LQTS cannot be investigated directly in human cardiomyocytes (CMs) because harvesting mature CMs is confounded by many factors, such as limitations in cell numbers and proliferative capacity. Thus, previous investigations of LQTS used heterologous expression in non-human CMs and animal models. However, heterologous systems do not precisely reflect the influence of potential compensatory pathways and the impact of known and unknown accessory channel subunits, all effects that may be present in functional CMs. Additionally, because of the profound differences between animal and humans in the biochemical, physiological and anatomical characteristics of CMs, animal models do not faithfully reproduce the pathophysiological features of human LQTS [3]. Therefore, as an increasing number of genetic variants become associated with LQTS, it is essential to develop effective and accurate model systems to understand the mechanism underlying LQTS. iPSC platforms to derive different cells and tissues in the human body for disease models appear to be an attractive option.

The LQTS-specific iPSC model was firstly established in LQT1 due to an autosomal dominant missense mutation (R190Q) in the KCNQ1 gene [4]. LQT1-derived iPSC-CMs maintained the disease phenotypes of LQT1. The action potential duration was markedly prolonged in iPSC-CMs from patients, as compared with cells from the control. Further characterization of the role of the mutation revealed a dominant negative trafficking defect associated with a 70%–80% reduction in I_{Ks} current. The iPSC models of LQTS were also obtained in other studies (Table 1). LQTS-derived iPSC lines can be differentiated into CMs and documented phenotypes that are indicative of LQTS, showing the disease's characteristic electrophysiological signature, establishing a convenient system for in vitro illustration of mechanisms underlying LQTS. Particularly, one obvious advantage of human iPSC-CMs is the possibility to evaluate the effect of the patient's genetic background on the relation between genotype and phenotype. In addition, access to LQTS-derived iPS-CMs in combination with other technologies presents the opportunity to identify disease-relevant biological characteristics that can shed light on new mechanistic insights into LQTS pathology not readily evident through conventional systems, making the LQTS-derived iPS-CMs a promising resource for more research work in the future (Fig. 1).

Current drug development programs are inefficient. Compounds that appear to be safe and efficacious in animal models or in vitro cell systems may fail in later clinical trials because of safety issues or a lack of efficacy [5]. iPSC technology provides the means to obtain drug efficacy and toxicity data in a disease-relevant context, which ensures lower attrition at late stages of the clinical pipeline. The ability to derive and test cells from individuals with known drug sensitivities would help identify the molecular basis of variable human drug responses. In addition, Patient-derived iPSCs are amenable to almost limitless expansion, thus enabling tests of more candidate compounds than possible in actual clinical trials. Moreover, testing drugs on LQTS-specific iPSCs also suggests the possibility for individualized medicine strategies and optimization of therapies of patient with a specific genetic background.

Table 1
Summary of existing induced pluripotent stem cell models of long QT syndrome.

Syndrome	Transcription factors	Affected gene	Gene mutation
LQT1	OCT3/4, SOX2, KLF4, and c-MYC	KCNQ1	R190Q
LQT2	(hOCT3/4, hSOX2, hKLF4 or		
hc-MYC	KCNH2 (HERG)	R176W	
LQT1	OCT3/4, SOX2, KLF4, and		
c-MYC	KCNQ1	1893delC	
LQT2	OCT4, SOX2 and KLF4	KCNH2 (HERG)	A614V
LQT2	OCT4, SOX2, LIN28, and NANOG	KCNH2 (HERG)	G1681A
LQT8	YFP, SOX2, OCT3/4, MYC or KLF4	ACNA1C gene	G406R mutation
LQT3	Oct4, Sox2, and Klf4 or c-Myc	SCN5A	△KPQ
LQT2	OCT4, SOX2, NANOG, LIN28, c-Myc, and KLF4	KCNH2 (HERG)	W1001X

* Corresponding authors.
E-mail addresses: pjq1980214@163.com (J. Pan), cfsun1@mail.xjtu.edu.cn (C. Sun).

ARTHRITIS & RHEUMATISM
Vol. 65, No. 6, June 2013, pp 1624–1635
DOI 10.1002/art.37933

FTY720 Ameliorates Murine Sclerodermatous Chronic Graft-Versus-Host Disease by Promoting Expansion of Splenic Regulatory Cells and Inhibiting Immune Cell Infiltration Into Skin

Doanh Le Huu, Takashi Matsushita, Guihua Jin, Yasuhito Hamaguchi, Minoru Hasegawa, Kazuhiko Takehara, and Manabu Fujimoto

Objective. **Sphingosine 1-phosphate (S1P) exerts a variety of activities in immune, inflammatory, and vascular systems. S1P plays an important role in systemic sclerosis (SSc) pathogenesis. Regulation of S1P in fibrotic diseases as well as in SSc was recently reported. FTY720, an oral S1P receptor modulator, has been shown to be a useful agent for the prevention of transplant rejection and autoimmune diseases. Murine sclerodermatous chronic graft-versus-host disease (GVHD) is a model for human sclerodermatous chronic GVHD and SSc. We undertook this study to investigate the effects of FTY720 in murine sclerodermatous chronic GVHD.**

Methods. **FTY720 was orally administered to allogeneic recipient mice from day 0 to day 20 (short-term, early-treatment group), from day 0 to day 42 (full-term, early-treatment group), or from day 22 to day 42 (delayed-treatment group) after bone marrow transplantation.**

Results. **Delayed administration of FTY720 attenuated, and early administration of FTY720 inhibited, the severity and fibrosis in murine sclerodermatous chronic GVHD. With early treatment, FTY720 induced expansion of splenic myeloid-derived suppressor cells, Treg cells, and Breg cells. Vascular damage in chronic GVHD was inhibited by FTY720 through down-regulating serum levels of S1P and soluble E-selectin. FTY720 inhibited infiltration of immune cells into skin. Moreover, FTY720 diminished the expression of messenger RNA for monocyte chemotactic protein 1, macrophage inflammatory protein 1α, RANTES, tumor necrosis factor α, interferon-γ, interleukin-6 (IL-6), IL-10, IL-17A, and transforming growth factor β1 in the skin.**

Conclusion. **FTY720 suppressed the immune response by promoting the expansion of regulatory cells and reducing vascular damage and infiltration of immune cells into the skin. Taken together, these results have important implications for the potential use of FTY720 in the treatment of sclerodermatous chronic GVHD and SSc in humans.**

Sphingosine 1-phosphate (S1P) is a biologically active lysophospholipid with key functions in the immune, inflammatory, and vascular systems (1–3). Fingolimod (FTY720) is phosphorylated by sphingosine kinase (4) to become FTY720 phosphate. FTY720 phosphate can bind to S1P receptor 1 ($S1P_1$), $S1P_3$, $S1P_4$, and $S1P_5$, but not to $S1P_2$ (1). These receptors are critically involved in cell survival, cytoskeletal rearrangements, cell motility, and cell migration (5). FTY720 has also been reported to accelerate the homing of lymphocytes from peripheral blood and spleen into secondary lymphoid tissues (6). In addition, FTY720 retains lymphocytes within the thymus and secondary lymphoid organs, eliminating their ability to home to peripheral sites of inflammation (7).

Moreover, recent reports indicate that FTY720 also modulates monocyte/macrophage migration and

Supported by grants-in-aid from the Ministry of Education, Science, and Culture of Japan.

Doanh Le Huu, MD, Takashi Matsushita, MD, PhD, Guihua Jin, MD, Yasuhito Hamaguchi, MD, PhD, Minoru Hasegawa, MD, PhD, Kazuhiko Takehara, MD, PhD, Manabu Fujimoto, MD, PhD: Kanazawa University, Kanazawa, Japan.

Address correspondence to Takashi Matsushita, MD, PhD, Department of Dermatology, Faculty of Medicine, Institute of Medical, Pharmaceutical, and Health Sciences, Kanazawa University, 13-1 Takaramachi, Kanazawa, Ishikawa 920-8641, Japan. E-mail: t-matsushita@derma.m.kanazawa-u.ac.jp.

Submitted for publication September 18, 2012; accepted in revised form March 5, 2013.

activation (8), dendritic cell trafficking and function (9), Treg cell activity (10,11), and marginal zone (MZ) B cell movement (12,13). FTY720 has been shown to be a useful agent for the prevention of transplant rejection, contact hypersensitivity, and autoimmune diseases (14–17). Recent studies provided evidence that S1P and S1P receptors might be mediators involved in development of fibrotic diseases as well as systemic sclerosis (SSc) (18–22). Serum levels of S1P were reported to increase in SSc patients (19). SSc-derived fibroblasts showed decreased expression of $S1P_1$ and $S1P_2$ and increased expression of $S1P_3$ as compared with normal fibroblasts. Furthermore, phosphorylation of Smad3 was increased by S1P via $S1P_1$ and $S1P_2$ in SSc fibroblasts (18,20). In SSc fibroblasts, the phosphatase and tensin homolog (PTEN) level was restored and matrix metalloproteinase 1 (MMP-1), Smad3 phosphorylation, and collagen levels were normalized by dihydrosphingosine 1-phosphate (20). However, both S1P and FTY720 were demonstrated to have similar profibrotic effects including Smad phosphorylation and collagen up-regulation and induced myofibroblast differentiation from healthy fibroblasts via $S1P_3$ (23).

Chronic graft-versus-host disease (GVHD) emerges from alloreactive reactions between donor-derived immune and host cell populations. Transplantation of B10.D2 mouse bone marrow (BM) and splenocytes across minor histocompatibility loci into sublethally irradiated BALB/c mouse recipients is a well-established animal model for human sclerodermatous chronic GVHD and SSc, which show many clinical similarities (24). Histologic analysis of the initial stages of SSc and murine sclerodermatous chronic GVHD showed infiltration of mononuclear cells into the dermis with an associated increase in collagen synthesis (25). In the present study, we analyzed the effects of FTY720 on murine sclerodermatous chronic GVHD.

MATERIALS AND METHODS

BM transplantation. Male B10.D2 (H-2^d) mice and female BALB/c (H-2^d) mice ages 8–12 weeks were used as donors and recipients, respectively. BM was depleted of T cells with anti-Thy1.2 microbeads (Miltenyi Biotec). BALB/c recipient mice were irradiated with 800 cGy (MBR-1520R; Hitachi) and were injected via the tail vein with 10×10^6 T cell–depleted BM cells and 10×10^6 splenocytes in 0.5 ml of phosphate buffered saline (PBS) to generate murine sclerodermatous chronic GVHD (allogeneic BM transplantation [BMT]). A control syngeneic group of female BALB/c mice received male BALB/c mouse T cell–depleted BM cells and splenocytes (syngeneic BMT). All studies were approved by the institutional review board.

Reagents. FTY720 (fingolimod; Cayman Chemical) was administered to allogeneic recipients by daily oral gavage at a dose of 1 mg/kg from day 0 to day 20 (short-term, early-treatment group), day 0 to day 42 (full-term, early-treatment group), or day 22 to day 42 (delayed-treatment group) after BMT. Control mice received distilled water only (allogeneic group).

GVHD skin score. The clinical chronic GVHD score was previously described (26): healthy appearance = 0; skin lesions with alopecia ≤ 1 cm^2 in area = 1; >1–2 cm^2 = 2; >2–5 cm^2 = 3; >5–10 cm^2 = 4; >10–15 cm^2 = 5; >15–20 cm^2 = 6; >20 cm^2 = 7. Additionally, animals were assigned 0.4 points for skin disease (lesions or scaling) on the tail and 0.3 points each for lesions on the ears and paws (minimum score = 0, maximum score = 8). Final scores for dead animals were kept in the data set for the remaining time points.

Histologic analysis. The skin and lung were fixed in 10% formalin and embedded in paraffin. Sections (6 μm in thickness) were stained with hematoxylin and eosin and Masson's trichrome. Skin histopathology was scored by a dermatopathologist (blinded to the experimental groups) on the basis of epidermal interface changes, dermal collagen thickness, mononuclear cell inflammation, subdermal fat loss, and follicular dropout, with scores from 0 to 2 for each category (total possible score 0–10) (27). Dermal thickness was defined as the thickness of skin from the top of the granular layer to the junction between the dermis and intradermal fat (28). Collagen deposition was quantified on trichrome-stained sections as the ratio of blue-stained area to total stained area using Adobe Photoshop CS4 analysis tools.

Sircol soluble collagen assay. Total soluble collagen was quantified using the Sircol Soluble Collagen Assay (Biocolor). Briefly, 6-mm skin and left lung samples were homogenized in acid–pepsin solution (0.5*M* acetic acid containing 1 mg/ml pepsin) over 2 nights at 4°C. After centrifugation, 1 ml of Sircol dye was added to 100 μl of supernatant and incubated for 30 minutes. After removing the suspension, droplets were dissolved in 1 ml Sircol alkali reagent, and relative absorbance was measured at 555 nm.

Immunohistochemical staining of skin. The skin samples were removed and frozen in liquid nitrogen using embedding medium for frozen tissue specimens (Tissue-Tek OCT compound; Sakura Finetek) and stored until used at −70°C. Frozen sections (6 μm) were immediately fixed in cold acetone and were incubated with rat anti-mouse CD3 monoclonal antibody (mAb) (17A2), rat anti-mouse CD4 mAb (GK1.5), rat anti-mouse CD11b mAb (M1-70), or rat anti-mouse B220 mAb (30-F11) (all from BD Biosciences). Rat IgG (Southern Biotech) was used as a control for nonspecific staining. Sections were then incubated sequentially (for 20 minutes at 37°C) with a biotinylated goat anti-rabbit IgG secondary antibody (BD Biosciences) followed by incubation with horseradish peroxidase–conjugated avidin–biotin complexes (Vector). Sections were washed 3 times with PBS between incubations, developed with 3,3′-diaminobenzidine tetrahydrochloride and H_2O_2, and then counterstained with methyl green.

Skin sections (6-μm thick) were applied to slides. Before immunostaining, the slides were heated at 37°C overnight in a drying oven and then deparaffinized in xylene, hydrated through graded alcohols, and washed in distilled water. For PTEN and MMP-1 detection, antigen retrieval was

performed via heat treatment (10 minutes in 10 mmoles/liter sodium citrate buffer at 95°C). The slides were allowed to cool for 20 minutes, then rinsed in distilled water and placed into a container of wash buffer (Tris buffered saline). Endogenous peroxidase activity was blocked by incubating the slides for 5 minutes in 3% H_2O_2. After rinsing in wash buffer, sections were incubated for 1 hour at room temperature with anti-PTEN antibody (1:100 dilution, NBP1-73972; Novus Biologicals), anti–MMP-1 antibody (1:100 dilution, NBP1-72209; Novus Biologicals), or antibody against Smad3 phosphorylated at Ser^{425} (1:100 dilution, NB100-92630; Novus Biologicals) in wash buffer. Slides were rinsed in wash buffer and incubated for 30 minutes with peroxidase-labeled donkey anti-rabbit IgG antibody (BD Biosciences) followed by incubation with avidin–biotin–peroxidase complexes (Vectastain ABC method; Vector). Sections were developed with 3,3′-diaminobenzidine tetrahydrochloride and H_2O_2 and then counterstained with methyl green.

Immunohistochemical stains were evaluated for the presence of positively staining fibroblast-like spindle cells between collagen bundles in the dermis. The following semiquantitative scale, based on the percentage of positively stained spindle cells, was used: − (no staining), + (<25% staining), ++ (25–50% staining), +++ (>50–75% staining), and ++++ (>75–100% staining).

Stained cells were counted under a high-power microscopic field (original magnification × 400) on a light microscope. Each section was examined and scored independently by 2 investigators in a blinded manner. The mean score was used for analysis.

Enzyme-linked immunosorbent assay (ELISA). Serum samples were measured for levels of S1P, soluble E-selectin, soluble intercellular adhesion molecule 1 (sICAM-1), and soluble vascular cell adhesion molecule 1 (sVCAM-1) using an S1P competitive ELISA kit (Echelon Biosciences) and Quantikine mouse soluble E-selectin, sICAM-1, and sVCAM-1 immunoassay kits (R&D Systems), respectively, according to the manufacturers' instructions.

Preparation of skin cell suspensions for flow cytometry. A 3 × 3–cm piece of depilated back skin was minced and then digested in 7 ml of RPMI 1640–10% fetal bovine serum (FBS) containing 2 mg/ml crude collagenase (Sigma-Aldrich), 1.5 mg/ml hyaluronidase (Sigma-Aldrich), and 0.03 mg/ml DNase I (Sigma-Aldrich) at 37°C for 90 minutes. Digested cells were passed through a 70-μm Falcon cell strainer (BD Biosciences) to generate single-cell suspensions. After centrifugation at 1,500 revolutions per minute for 5 minutes, the pellet was resuspended in 70% Percoll solution (GE Healthcare) and then overlaid with 37% Percoll solution, followed by centrifugation at 1,800 rpm for 20 minutes. The cells were aspirated from the Percoll interface and passed through a 70-μm Falcon cell strainer. The cells were harvested by centrifugation and washed with PBS plus 5% FBS.

Flow cytometry. The following mAb to mouse antigens were used: fluorescein isothiocyanate (FITC)–conjugated, phycoerythrin (PE)–conjugated, PE–Cy5–conjugated, PE–Cy7–conjugated, PerCP–Cy5.5–conjugated, allophycocyanin (APC)–conjugated, and APC–Cy7–PE–Cy7–conjugated anti-B220 (30-F11), APC–Cy7–conjugated anti-CD4 (RM4-5), Pacific Blue–conjugated anti-CD8 (53-6.7), FITC-conjugated anti-CD11b (M1-70), PerCP–Cy5.5–conjugated anti-CD11c (N418), PE–Cy7–conjugated anti-CD19 (1D3), PE-conjugated anti-CD25 (MF-14), and FITC-conjugated anti–Gr-1 (RB6-8C5) (all from BioLegend), PE-conjugated anti-$S1P_1$ (713412; R&D Systems), and FITC-conjugated anti-FoxP3 (FJK-16s; eBioscience). The Live/Dead Fixable Aqua Dead Cell Stain kit was from Invitrogen. Splenic and skin single-cell suspensions were stained for 20 minutes for 3- to 6-color immunofluorescence analysis at 4°C using mAb at predetermined optimal concentrations. Intracellular staining for FoxP3 was performed using the Cytofix/Cytoperm kit (BD Biosciences). Stained samples were analyzed on a FACSCanto II (BD Biosciences). Data were analyzed using FlowJo software (Tree Star).

Intracellular cytokine staining. Cell suspensions were stimulated for 5 hours at 37°C with lipopolysaccharide (10 μg/ml; Sigma-Aldrich), phorbol myristate acetate (PMA) (50 ng/ml; Sigma-Aldrich), ionomycin (500 ng/ml; Sigma-Aldrich), and brefeldin A (3 μ*M*; BioLegend) for detection of interleukin-10 (IL-10) production by B cells, and were stimulated for 4 hours at 37°C with PMA (50 ng/ml), ionomycin (1 μg/ml), and brefeldin A (3 μ*M*) for detection of cytokine production by T cells. After cell surface staining, the cells were washed, fixed, and permeabilized using the Cytofix/Cytoperm kit, then stained with anti–IL-10 mAb (JES5-16E3) or with anti–tumor necrosis factor α (anti-TNFα) (MP6-XT22), anti–interferon-γ (anti-IFNγ) (XMG1.2), or anti–IL-17A (TC11-18H10.1) (all from BioLegend).

Reverse transcription–polymerase chain reaction (RT-PCR). Total RNA was isolated from frozen skin specimens using RNeasy spin columns (Qiagen) and digested with DNase I (Qiagen) to remove chromosomal DNA. Total RNA was reverse-transcribed to a complementary DNA using a reverse transcription system with random hexamers (Promega). Cytokine messenger RNA (mRNA) was analyzed using real-time quantitative RT-PCR (Applied Biosystems). Real-time RT-PCR was performed on an ABI Prism 7000 sequence detector (Applied Biosystems). GAPDH was used to normalize the mRNA. The relative expression of real-time RT-PCR products was determined according to the $\Delta\Delta C_t$ method to compare target gene and GAPDH mRNA expression.

CD4+ T cell proliferation assay. Splenic CD11b+ cells were isolated from syngeneic BM-transplanted, FTY720-treated, and water-treated allogeneic BM-transplanted mice 7 days after BMT, and splenic CD4+ T cells were isolated from wild-type B10.D2 mice, using corresponding MACS magnetic microbeads (Miltenyi Biotec). Isolated CD4+ T cells were labeled with 10 μ*M* 5,6-carboxyfluorescein succinimidyl ester (CFSE; Invitrogen). CFSE-labeled CD4+ T cells (4×10^5) were cocultured with various amounts of purified CD11b+ cells in the presence of plate-bound anti-CD3 (1 μg/ml) and anti-CD28 (1 μg/ml) for 48 hours in 24-well plates. Two-color flow cytometric analyses were performed.

Statistical analysis. All data are shown as the mean ± SEM. The significance of differences between sample means was determined with Student's *t*-test.

RESULTS

Delayed administration of FTY720 attenuates and early administration of FTY720 inhibits murine sclerodermatous chronic GVHD. When compared with the water-treated group, full-term early treatment with FTY720 significantly inhibited murine sclerodermatous